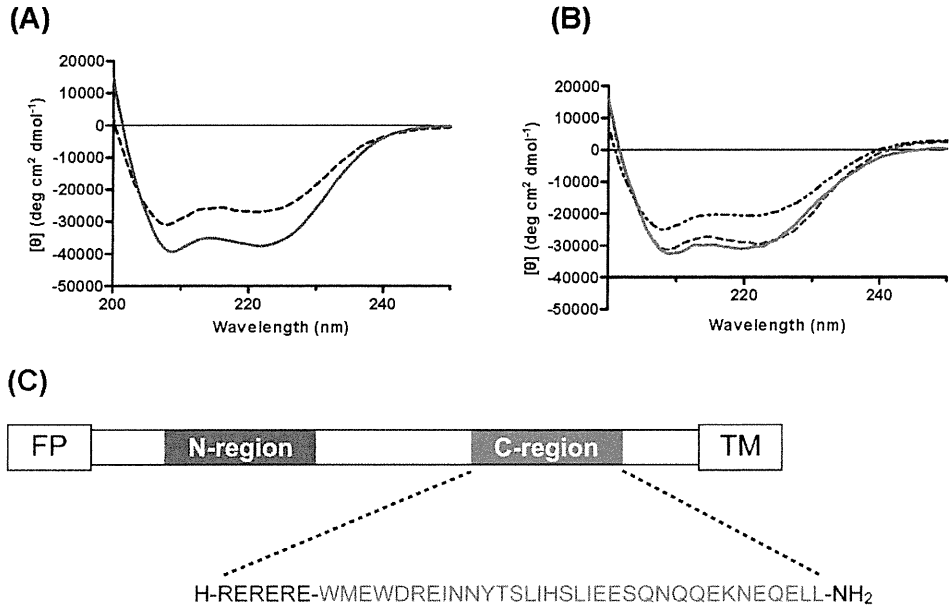

Figure 3. (A) Circular dichroism (CD) spectra of N36RE and triN36e. In the spectra, a blue dashed line and a green line show N36RE (monomer) and triN36e (trimer), respectively. Concentrations of the peptides are 10 and 3.3 μM for N36RE and triN36e, respectively. (B) CD spectra in the presence or absence of C34RE peptide. The spectra show the following: a dashed green line, triN36e; a dashed blue line, C34RE; a red line, triN36e+C34RE, respectively. The concentrations of peptides were as follows: triN36e (2.3 μM), C34-derived peptide C34RE (7 μM), and mixture of both peptides (3.5 μM each). (C) The amino acid sequence of C34RE described in single letters. FP and TM represent hydrophobic fusion peptide and transmembrane domain, respectively.

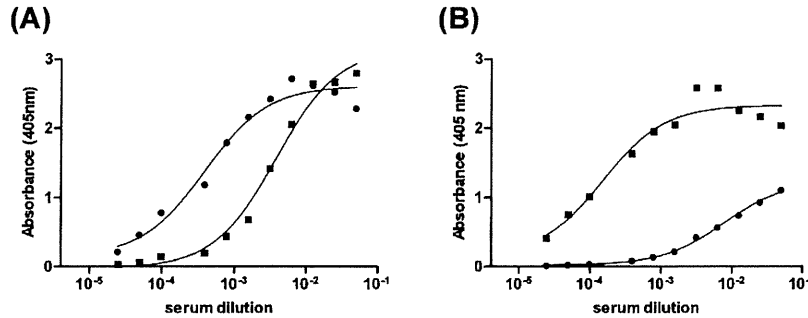

Figure 4. Serum titers of antibodies produced by N36 monomer and conformationally constrained N36 trimeric antigen. The titers were evaluated against N36RE (monomer) (A) and triN36e (trimer) (B). The plots indicate the results of sera obtained from N36RE-immunized mouse (•) and triN36e-immunized mouse (■).

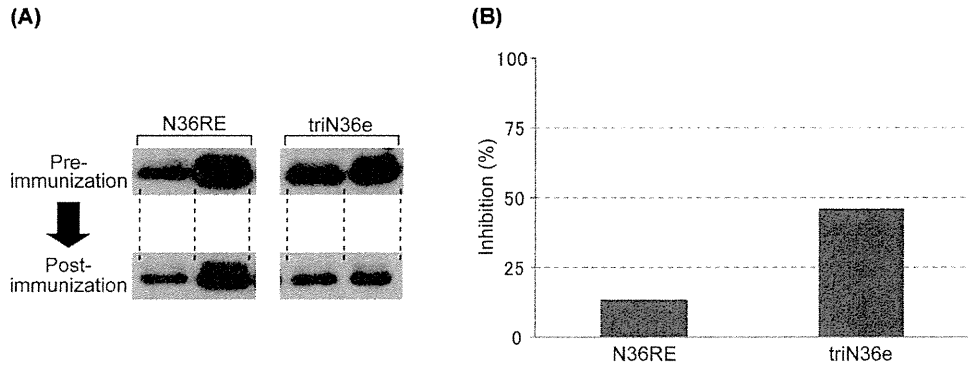

Figure 5. Determination of neutralization activity of the antibodies produced by immunization of peptidomimetic antigens. (A) Results of p24 assay to evaluate inhibition for HIV-1 infection by produced antibodies. Preimmunization sera were used as control. Experiments were duplicated. (B) Average % inhibition of p24 production calculated from the band intensities in panel (A).

of structure-specific antibody is still not clear, but the results could suggest the efficacy of producing antibodies with structural specificity and that the synthesis of structure-involving antigens is an effective strategy when higher specificity is required.

Neutralizing activity of sera against HIV-1 infection was assessed by p24 assays utilizing antisera from two mice that showed antibody production for each antigen (Figure 5). Sera

Table 1. Differences of α-Helicities between N36RE and triN36e Calculated from CD Spectra in Figure [3]

	$[\theta]_{222}$	$[\theta]_{222}/[\theta]_{208}$	α-helicity
N36RE	−30 957	0.87	73%
triN36e	−38 998	0.96	95%

Table 2. EC_{50} and CC_{50} Values Calculated from Inhibition Assays of Peptidomimetics

	AZT	triN36e	N36RE
EC_{50} (μM)[a]	0.047	0.49	1.4
CC_{50} (μM)[b]	>50	>1	>10

[a] EC_{50} values are based on the inhibition of HIV-induced cytopathogenicity in MT-4 cells. [b] CC_{50} values are based on the reduction of the viability of MT-4 cells. All data are the mean values for at least three experiments.

from mice immunized with the same antigen showed similar inhibitory activity against viral infection (12.5% and 14.8% for N36RE, 40.3% and 52.1% for triN36e). A trend was observed that the sera from triN36e immunization shows higher inhibition than those from N36RE immunization. This suggests that the synthetic antigen corresponding to the N36 trimeric form induces antibody with neutralization activity superior to that of the monomer peptide antigen and implies a restricted response of B-cells upon immunization to the trimeric form of N36RE. In order to assess the compatibility of induced antibodies in HIV-1 entry inhibition, the HIV-1 inhibitory activities of peptidomimetics (N36RE and triN36e) have been evaluated by viral infection and cytotoxicity assays. A C-terminal region peptide known as Enfuvirtide (T20, Roche/Trimeris) has been used clinically as a fusion inhibitor, and its success indicates that gp41-derived peptides might be potent inhibitors, useful against HIV-1 infection (*30*). In the development of anti-HIV peptides, several mimetics such as Enfuvirtide, CD4 binding site of gp120 (*31*), and protein-nucleic acid interactions (*32*), which disrupt protein−protein interactions, have been produced. As indicated in Table 2, N36 and triN36e showed modest inhibitory activity as reported in previous studies (*33*−*35*). The potency of triN36e was three times higher than that of N36RE indicating that the active structure of monomer N36RE is a trimeric form. Cytotoxicity of the antigens was not observed at concentrations of 1 μM of triN36e and 10 μM of N36RE.

CONCLUSIONS

In summary, a mimic of HIV-1 gp41-N36 designed as a new vaccine has been synthesized utilizing a novel template with three branched linkers of equal lengths. Thiazolidine-forming ligation attached the esteraldehyde of three-branched template with N-terminal cysteine of peptides in an aqueous medium. The resulting peptide antigen successfully induces antibodies with neutralization activity against HIV-1 infection. It is of special interest that the antibody produced acquires structural preference to antigen, which showed 30 times higher binding affinity for trimer than for monomer. This indicates the effectiveness of the design based on the structural dynamics of HIV-1 fusion mechanism of an antigen which could elicit neutralizing antibodies. In a design based on the N36 region of gp41, the exposed timing of epitopes is limited during HIV-1 entry (*36*), and carbohydrates, which could make accession of antibodies to epitopes difficult, are not associated with the amino acid residues of the native protein. These two advantages could further enhance the potential of a vaccine design based on the N36 region. During preparation of the manuscript, a new HIV vaccine strategy was reported by Burton's group (*37*). The report describes the importance of antibody recognition for the trimer form of surface protein. The trimer-specific antibodies indicate broad and potent neutralization. The gp41 trimer-form specific antibody produced in this study could also obtain the corresponding properties. The elucidation of antibody-producing mechanisms and epitope recognition mode of antibodies in antiserum during HIV-1 entry will be addressed in future studies.

ACKNOWLEDGMENT

The authors deeply thank Prof. K. Akiyoshi (Tokyo Medical and Dental Univ.) for allowing access to CD spectroporalimeter.

Supporting Information Available: HPLC chromatograms and NMR charts of compounds **3**, **5**, and **6**. Results of ESI-TOF-MS, and HPLC chromatograms of peptides N36RE, N36REGC, and triN36e. Results of serum titer ELISA of antisera collected during immunization. This material is available free of charge via the Internet at http://pubs.acs.org.

LITERATURE CITED

(1) Cabezas, E., Wang, M., Parren, P. W. H. I., Stanfield, R. L., and Satterthwait, A. C. (2000) A structure-based approach to a synthetic vaccine for HIV-1. *Biochemistry 39*, 14377–14391.

(2) Burton, D. R., Barbas, C. F., III, Persson, M. A. A., Koenig, S., Chanock, R. M., and Lerner, R. A. (1991) A large array of human monoclonal antibodies to type 1 human immunodeficiency virus from combinatorial libraries of asymptomatic seropositive individuals. *Proc. Natl. Acad. Sci. U.S.A. 88*, 10134–10137.

(3) Conley, A. J., Kessler, J. A. II, Boots, L. J., Tung, J. S., Arnold, B. A., Keller, P. M., Shaw, A. R., and Emini, R. A. (1994) Neutralization of divergent human immunodeficiency virus type 1 variants and primary isolates by IAM-41−2F5, an anti-gp41 human monoclonal antibody. *Proc. Natl. Acad. Sci. U.S.A. 91*, 3348–3352.

(4) Ofek, G., Tang, M., Sambor, A., Katinger, H., Mascola, J. R., Wyatt, R., and Kwong, P. D. (2004) Structure and mechanistic analysis of the anti-human immunodeficiency virus type 1 antibody 2F5 in complex with its gp41 epitope. *J. Virol. 78*, 10724–10737.

(5) Alam, S. M., McAdams, M., Boren, D., Rak, M., Scearce, R. M., Gao, F., Camacho, Z. T., Gewirth, D., Kelsoe, G., Chen, P., and Haynes, B. F. (2007) The role of antibody polyspecificity and lipid reactivity in binding of broadly neutralizing anti-HIV-1 envelope human monoclonal antibodies 2F5 and 4E10 to glycoprotein 41 membrane proximal envelope epitopes. *J. Immunol. 178*, 4424–4435.

(6) Nelson, J. D., Brunel, F. M., Jensen, R., Crooks, E. T., Cardoso, R. M. F., Wang, M., Hessell, A., Wilson, I. A., Binley, J. M., Dawson, P. E., Burton, D. R., and Zwick, M. B. (2007) An affinity-enhanced neutralizing antibody against the membrane-proximal external region of human immunodeficiency virus type 1 gp41 recognizes an epitope between those of 2F5 and 4E10. *J. Virol. 81*, 4033–4043.

(7) Cardoso, R. M. F., Zwick, M. B., Stanfield, R. L., Kunert, R., Binley, J. M., Katinger, H., Burton, D. R., and Wilson, I. A. (2005) Broadly neutralizing anti-HIV antibody 4E10 recognizes a helical conformation of a highly conserved fusion-associated motif in gp41. *Immunity 22*, 163–173.

(8) Trkola, A., Purtscher, M., Muster, T., Ballaun, C., Buchacher, A., Sullivan, N., Srinivasan, K., Sodroski, J., Moore, J. P., and Katinger, H. (1996) Human monoclonal antibody 2G12 defines a distinctive neutralization epitope on the gp120 glycoprotein of human immunodeficiency virus type 1. *J. Virol. 70*, 1100–1108.

(9) Pantophlet, R., Saphire, E. O., Poignard, P., Parren, P. W. H. I., Wilson, I. A., and Burton, D. R. (2003) Fine mapping of the interaction of neutralizing and nonneutralizing monoclonal antibodies with the CD4 binding site of human immunodeficiency virus type 1 gp120. *J. Virol. 77*, 642–658.

(10) Sanders, R. W., Vesanen, M., Schuelke, N., Master, A., Schiffner, L., Kalyanaraman, R., Paluch, M., Berkhout, B., Maddon, P. J., Olson, W. C., Lu, M., and Moore, J. P. (2002) Stabilization of the soluble, cleaved, trimeric form of the envelope glycoprotein complex of human immunodeficiency virus type 1. *J. Virol. 76*, 8875–8889.

(11) Yang, X., Wyatt, R., and Sodroski, J. (2001) Improved elicitation of neutralizing antibodies against primary human immunodeficiency viruses by soluble stabilized envelope glycoprotein trimers. *J. Virol. 75*, 1165–1171.

(12) Grundner, C., Mirzabekov, T., Sodroski, J., and Wyatt, R. (2002) Solid-phase proteoliposomes containing human immunodeficiency virus envelope glycoproteins. *J. Virol. 76*, 3511–3521.

(13) De Rosny, E., Vassell, R., Wingfield, R. T., Wild, C. T., and Weiss, C. D. (2001) Peptides corresponding to the heptad repeat motifs in the transmembrane protein (gp41) of human immunodeficiency virus type 1 elicit antibodies to receptor-activated conformations of the envelope glycoprotein. *J. Virol. 75*, 8859–8863.

(14) Tam, J. P., and Yu, Q. (2002) A facile ligation approach to prepare three-helix bundles of HIV fusion-state protein mimetics. *Org. Lett. 4*, 4167–4170.

(15) Xu, W., and Taylor, J. W. (2007) A template-assembled model of the N-peptide helix bundle from HIV-1 gp-41 with high affinity for C-peptide. *Chem. Biol. Drug Des. 70*, 319–328.

(16) Louis, J. M., Nesheiwat, I., Chang, L., Clore, G. M., and Bewlet, C. A. (2003) Covalent trimers of the internal N-terminal trimeric coiled-coil of gp41 and antibodies directed against them are potent inhibitors of HIV envelope-mediated cell fusion. *J. Biol. Chem. 278*, 20278–20285.

(17) Chen, Y.-H., Yang, J. T., and Chau, K. H. (1974) Determination of the helix and β form of proteins in aqueous solution by circular dichroism. *Biochemistry 13*, 3350–3359.

(18) Gans, P. J., Lyu, P. C., Manning, M. C., Woody, R. W., and Kallenbach, N. R. (1991) The helix-coil transition in heterogeneous peptides with specific side-chain interactions: theory and comparison with CD spectral data. *Biopolymers 13*, 1605–1614.

(19) Jackson, D. Y., King, D. S., Chmielewski, J., Singh, S., and Schultz, P. G. (1991) A general approach to the synthesis of short alpha-helical peptides. *J. Am. Chem. Soc. 113*, 9391–9392.

(20) Ohba, K., Ryo, A., Dewan, M. Z., Nishi, M., Naito, T., Qi, X., Inagaki, Y., Nagashima, Y., Tanaka, Y., Okamoto, T., Terashima, K., and Yamamoto, N. (2009) Follicular dendritic cells activate HIV-1 replication in monocytes/macrophages through a juxtacrine mechanism mediated by P-selectin glycoprotein ligand 1. *J. Immunol. 183*, 524–532.

(21) Liu, J., Shu, W., Fagan, M. B., Nunberg, J. H., and Lu, H. (2001) Structural and functional analysis of the HIV gp41 core containing an Ile573 to Thr substitution: implications for membrane fusion. *Biochemistry 40*, 2797–2807.

(22) Liu, C. F., and Tam, J. P. (1994) Peptide segment ligation strategy without use of protecting groups. *Proc. Natl. Acad. Sci. U.S.A. 91*, 6584–6588.

(23) Tam, J. P., and Miao, Z. (1999) Stereospecific pseudoproline ligation of N-terminal serine, threonine, or cysteine-containing unprotected peptides. *J. Am. Chem. Soc. 121*, 9013–9022.

(24) Tam, J. P., Yu, Q., and Yang, J.-L. (2001) Tandem ligation of unprotected peptides through thiaprolyl and cysteinyl bonds in water. *J. Am. Chem. Soc. 123*, 2487–94.

(25) Eom, K. D., Miao, Z., Yang, J.-L., and Tam, J. P. (2003) Tandem ligation of multipartite peptides with cell-permeable activity. *J. Am. Chem. Soc. 125*, 73–82.

(26) Sadler, K., Zhang, Y., Xu, J., Yu, Q., and Tam, J. P. (2008) Quaternary protein mimetics of gp41 elicit neutralizing antibodies against HIV fusion-active intermediate state. *Biopolym. (Pept. Sci.) 90*, 320–329.

(27) Bychkova, V. E., Dujsekina, A. E., Klenin, S. I., Tiktopulo, E. I., Uversky, V. N., and Ptitsyn, O. B. (1996) Molten globule-like state of cytochrome *c* under conditions simulating those near the membrane surface. *Biochemistry 35*, 6058–6063.

(28) Nishi, K., Komine, Y., Sakai, N., Maruyama, T., and Otagiri, M. (2005) Cooperative effect of hydrophobic and electrostatic forces on alcohol-induced α-helix formation of α_1-acid glycoprotein. *FEBS Lett. 579*, 3596–3600.

(29) Chan, D. C., Chutkowski, C. T., and Kim, P. S. (1998) Evidence that a prominent cavity in the coiled coil of HIV type 1 gp41 is an attractive drug target. *Proc. Natl. Acad. Sci. U.S.A. 95*, 15613–15617.

(30) Liu, S., Jing, W., Cheng, B., Lu, H., Sun, J., Yan, X., Niu, J., Farmar, J., Wu, S., and Jiang, S. (2007) HIV gp41 C-terminal heptad repeat contains multifunctional domains: relation to mechanism of action of anti-HIV peptides. *J. Biol. Chem. 282*, 9612–9620.

(31) Franke, R., Hirsch, T., Overwin, H., and Eichler, J. (2007) Synthetic mimetics of the CD4 binding site of HIV-1 gp120 for the design of immunogens. *Angew. Chem., Int. Ed. 46*, 1253–1255.

(32) Robinson, J. A. (2008) β-hairpin peptidomimetics: design, structures and biological activities. *Acc. Chem. Res. 41*, 1278–1288.

(33) Lu, M., Ji, H., and Shen, S. (1999) Subdomain folding and biological activity of the core structure from human immunodeficiency virus type 1 gp41: implications for viral membrane fusion. *J. Virol. 73*, 4433–4438.

(34) Eckert, D. M., and Kim, P. S. (2001) Design of potent inhibitors of HIV-1 entry from the gp41 N-peptide region. *Proc. Natl. Acad. Sci. U.S.A. 98*, 11187–11192.

(35) Bianchi, E., Finotto, M., Ingallinella, P., Hrin, R., Carella, A. V., Hous, X. S., Schleif, W. A., and Miller, M. D. (2005) Covalent stabilization of coiled coils of the HIV gp41 N region yields extreamely potent and broad inhibitors of viral infection. *Proc. Natl. Acad. Sci. U.S.A. 102*, 12903–12908.

(36) Zwick, M. B., Saphire, E. O., and Burton, D. R. (2004) gp41: HIV's shy protein. *Nat. Med. 10*, 133–134.

(37) Walker, L. M., Phogat, S. K., Chan-Hui, P.-Y., Wagner, D., Phung, P., Goss, J. L., Wrin, T., Simek, M. D., Fling, S., Mitcham, J. L., Lehrman, J. K., Priddy, F. H., Olsen, O. A., Frey, S. M., Hammond, P. W., Kaminsky, S., Zamb, T., Moyle, M., Koff, W. C., Poignard, P., and Burton, D. R. (2009) Broad and potent neutralizing antibodies from an African donor reveal a new HIV-1 vaccine target. *Science 326*, 285–289.

BC900502Z

INDUCTION OF MYOGENIC DIFFERENTIATION BY SDF-1 VIA CXCR4 AND CXCR7 RECEPTORS

ROBERTA MELCHIONNA, PhD,[1] ANNA DI CARLO, PhD,[1] ROBERTA DE MORI, PhD,[1] CLAUDIA CAPPUZZELLO, PhD,[1] LAURA BARBERI, PhD,[2] ANTONIO MUSARÒ, PhD,[2] CHIARA CENCIONI, BS,[1] NOBUTAKA FUJII, PhD,[3] HIROKAZU TAMAMURA, PhD,[4] MARCO CRESCENZI, MD,[5] MAURIZIO C. CAPOGROSSI, MD,[1] MONICA NAPOLITANO, MD,[1] and ANTONIA GERMANI, MD[1,6]

[1] Laboratorio di Patologia Vascolare, Istituto Dermopatico dell'Immacolata, Istituto di Ricovero e Cura a Carattere Scientifico, Via Monti di Creta 104, Rome 00167, Italy
[2] Department of Histology and Medical Embryology, University of Rome La Sapienza, Rome, Italy
[3] Graduate School of Pharmacological Science, Kyoto University, Kyoto, Japan
[4] Tokyo Medical and Dental University, Tokyo, Japan
[5] Department of Environment and Primary Prevention, Istituto Superiore di Sanità, Rome, Italy
[6] Fondazione Livio Patrizi, Rome, Italy

Accepted 2 November 2009

ABSTRACT: The stromal cell–derived factor (SDF)-1/CXC receptor 4 (CXCR4) axis has been shown to play a role in skeletal muscle development, but its contribution to postnatal myogenesis and the role of the alternate SDF-1 receptor, CXC receptor 7 (CXCR7), are poorly characterized. Western blot analysis and real-time polymerase chain reaction (PCR) were performed to evaluate in vitro the effect of SDF-1 and CXCR4 and CXCR7 inhibition on myogenic differentiation. Proliferating myoblasts express CXCR4, CXCR7, and SDF-1; during myogenic differentiation, CXCR4 and CXCR7 levels are downregulated, and SDF-1 release is decreased. SDF-1 anticipates myosin heavy chain accumulation and myotube formation in both C2C12 myoblasts and satellite cells. Interestingly, inhibition of CXCR4 and CXCR7 signaling, either by drugs or RNA interfererence, blocks myogenic differentiation. Further, the CXCR4 antagonist, 4F-benzoyl-TN14003, inhibits myoblast cell cycle withdrawal and decreases the retinoblastoma gene (pRb) product accumulation in its hypophosphorylated form. Our experiments demonstrate that SDF-1 regulates myogenic differentiation via both CXCR4 and CXCR7 chemokine receptors.

Muscle Nerve **41:** 828–835, 2010

The chemokine, stromal cell–derived factor (SDF)-1, and its receptor, CXC receptor 4 (CXCR4), control hematopoietic progenitor cell migration and differentiation as well as several aspects of stem cell function, including stem cell trafficking and development. Indeed, both SDF-1 and CXCR4 knockout mice die in utero and show a shared phenotype of impaired B-cell lymphopoiesis and bone marrow myelopoiesis.[1–3] Further, CXCR4 and SDF-1 deletion affects neuronal precursor cell migration. This produces abnormalities of cerebellar and hippocampal morphology and cardiac defects.[1,3–6] The SDF-1/CXCR4 axis plays a role in vasculature formation[7] and promotes angiogenesis both in vitro and in vivo.[8,9] SDF-1/CXCR4 has been considered to be a unique ligand–receptor pair, but recently the orphan receptor, RDC1, named CXC receptor 7 (CXCR7),[10] was shown to function as an alternate SDF-1 receptor that has both shared and distinct functions from CXCR4.[11–14] Specifically, CXCR7 activity promotes tumor growth in animal models,[11] is involved in renal progenitor cell engraftment into injured areas in an animal model of acute renal failure,[14] and plays a role in cardiac development.[13]

SDF-1 signaling has an important role in skeletal muscle development. In fact, myogenic precursor cells that express CXCR4 migrate into limbs along SDF-1 gradients, where they differentiate and give origin to myofibers.[15] Reduced numbers of progenitor cells are found in the distal limb of CXCR4-deficient mice at an early stage of development (E10.5). At later stages (>E14), these mice exhibit severe defects of limb myogenesis, as demonstrated by a reduction of limb musculature.[16]

Although it is known that SDF-1 attracts CXCR4-expressing immune cells during the regenerative process, its involvement in modulating adult skeletal muscle function has been only partially characterized.[17–19] The role of the alternate SDF-1 receptor CXCR7 in myogenesis has not yet been investigated.

Herein we report that proliferating myoblasts express both CXCR4 and CXCR7. Moreover, they release SDF-1 in the culture medium. During myogenic differentiation such molecules are downregulated. We further demonstrate that SDF-1 treatment anticipates muscle differentiation and show that both CXCR4 and CXCR7 receptor signaling is involved in this process.

METHODS

Cell Culture. The murine myoblast C2C12 line was cultured in Dulbecco's modified Eagle medium

Abbreviations: 4FTN, 4F-benzoyl-TN14003; BrdU, bromodeoxyuridine; CM, conditioned medium; DM, differentiation medium; DMEM, Dulbecco's modified Eagle medium; ELISA, enzyme-linked immunoassay; ECL, electrochemiluminsecence; Erk, extracellular signal–related kinase; FCS, fetal calf serum; GADPH, glyceraldehyde-3-phosphate dehydrogenase; GM, growth medium; IGF-1, insulin-like growth factor 1; MAb, monoclonal antibody; MRF4, muscle regulatory factor 4; Myf5, myogenic regulatory factor 5; MyHC, myosin heavy chain MAb; MyoD, myogenic differentiation factor 1; RT-PCR, reverse transcription–polymerase chain reaction; SDF-1, stromal cell–derived factor-1; siRNA, small interfering RNA; PAb, polyclonal antibody; PE, phycoerythrin

Key words: chemokine; myogenesis; regeneration; satellite cells; SDF-1

Correspondence to: A. Germani; e-mail: antoniagermani@idi.it
Drs Melchionna and Di Carlo contributed equally to this article.

Published online 11 February 2010 in Wiley InterScience (www.interscience.wiley.com). DOI 10.1002/mus.21611

(DMEM) supplemented with 20% fetal calf serum (FCS; Euroclone, Inc., Milan, Italy) and antibiotics. In order to induce differentiation, cells at 70–80% confluence were shifted to DMEM supplemented with 2% horse serum (differentiation medium, or DM). SDF-1 was supplemented, at 100 ng/ml, when switching to DM. Peptide inhibitor, 4F-benzoyl-TN14003 (4FTN), and control scrambled peptide were kindly provided by Professor N. Fujii (Graduate School of Pharmacological Science Kyoto University) and Prof. H. Tamamura (Tokyo Medical and Dental University, Japan). The CXCR4 antagonist, AMD3100, was obtained from Sigma (St. Louis, Missouri). The CXCR7 antagonists, CCX754 and CCX733, were kindly provided by Dr. T. Schall (Chemocentryx, Mountain View, California). Primary satellite cells were isolated from C57BL/10SnJ mice, 4 weeks of age, and cultured as described elsewhere.[20]

mRNA Expression and Real-Time Reverse Transcription–Polymerase Chain Reaction (RT-PCR). Total RNA was converted to cDNA by reverse transcription (SuperScript First-Strand cDNA Synthesis; Invitrogen, Carlsbad, California), according to the manufacturer's instructions. mRNA expression levels were calculated by the Comparative cT Method (Applied Biosystems, San Mateo, California). The following primers were used: CXCR4, 5′-TTGCCGACTATGC CAGTCAA-3′ and 5′- CCGGGATGAAAACGTCCAT-3′; 5′-GGAAGCCCTGAGGTCACTTG-3′ and 5′-AGT AGTTGCCCAGGCTCTGCATAGT-3′; SDF-1, 5′-CA CTCCAAACTGTGCCCTTCA-3′ and 5′-CACTTTAGC TTCGGGTCAATGC-3′; glyceraldeyde-3-phosphate dehydrogenase (GAPDH), 5′-GGTCCTCA GTGTA GCCCAAGAT-3′ and 5′-TGCCAAGTATGATGACAT CAAGAAG-3′. Normalization was performed using GAPDH expression levels, and mRNA expression was determined by the $2^{-\Delta\Delta Ct}$ method. The amplicon size was 80 pb. The accession numbers of the genes are NM013655.3 (SDF-1), NM009911.3 (CXCR4), and NM007722.3 (CXCR7).

Western Blot Analysis. Cell extracts and Western blot analysis were performed as described elsewhere.[20] Membranes were probed with 0.4 μg/ml rabbit anti-MyoD polyclonal antibodies (PAb; BD PharMingen, San Diego, California), anti-myogenin monoclonal antibodies (MAb; Santa Cruz Biotechnology, Santa Cruz, California), anti–myosin heavy chain (anti-MyHC; 1:40, MF20), 0.5 μg/ml rabbit anti-CXCR4 or 0.5 μg/ml rabbit anti-CXCR7 PAb (Abcam, Cambridge, UK), anti-Rb (c-15; Santa Cruz Biotechnology), Erk1/2 and pErk1/2 (Cell Signaling Technology, Inc., Beverly, Massachusetts), and α-tubulin MAb (Oncogene Science, Inc., Cambridge, Massachusetts), followed by horseradish peroxidase–coupled secondary antibodies, and then developed by electrochemiluminescence (ECL; Amersham Pharmacia Biotech).

Flow Cytometric Analysis. C2C12 cells, grown either in growth medium (GM) or differentiation medium (DM) for 2 days were incubated in phosphate-buffered saline (PBS) containing 5% fetal calf serum (FCS) for 20 minutes at 4°C with phycoerthythrin (PE)-conjugated anti-CXCR4 MAb 1D9 (BD PharMingen). PE-conjugated rat immunoglobulin G2a was used as isotype control (BD PharMingen). Samples were analyzed by flow cytometry (FACScalibur, Becton Dickinson, San Jose, California) using CellQuest software.

SDF-1α Immunoassays. SDF-1α levels were measured using an enzyme-linked immunoassay (ELISA) assay (R&D Systems, Inc., Minneapolis, Minnesota), according to manufacturer's instructions. C2C12 cells plated in 60-mm dishes (10^5 cells/dish) were cultured in either GM for 1 day or DM for 1, 2, or 3 days. Conditioned medium was collected at the indicated time-points and concentrated 5 times with Centricon-3 microconcentrators (Millipore, Bedford, Massachusetts). Samples were assayed in triplicate and normalized by the Bradford method (Bio-Rad, Hercules, California).

Small Interfering RNA (siRNA) Knockdown of Gene Expression. C2C12 cells were grown to 50% confluence and transfected with 100 nM siRNAs using Lipofectamine (Invitrogen). The siRNAs were purchased from Santa Cruz Biotechnology (SDF-1 sc39368; CXCR4 sc35421; CXCR7 sc142643) together with a non-targeting control. Knockdown efficacy was determined 48 hours after transfection through measurement of SDF-1 into the cell supernatant by ELISA, and CXCR4 and CXCR7 protein levels by Western blot.

Luciferase Assay. C2C12 cells were transfected in GM with 0.5 μg of the reporter plasmid containing the luciferase gene under the transcriptional control of the myosin creatine kinase promoter (pMCK-Luc) together with 0.5 μg of pCMV-β-galactosidase (pCMV-β-gal). After 24 hours, cells were transferred to DM for another 24 hours. Then cells were harvested and lysed in 100 μl of 1× luciferase lysis buffer (Promega Italia). Luciferase activity was determined in triplicate and expressed as arbitrary units (AU). Transfection efficiency was normalized by correcting luciferase activity for the levels of β-gal protein.

Cell Cycle Analysis. To test bromodeoxyuridine (BrdU) incorporation, C2C12 cells were plated in GM for 24 hours at 2×10^5 cells per 60-mm plate and then transferred into DM for 2 days, either in the presence of 4FTN or control peptide. Cells were then exposed to media containing BrdU (30

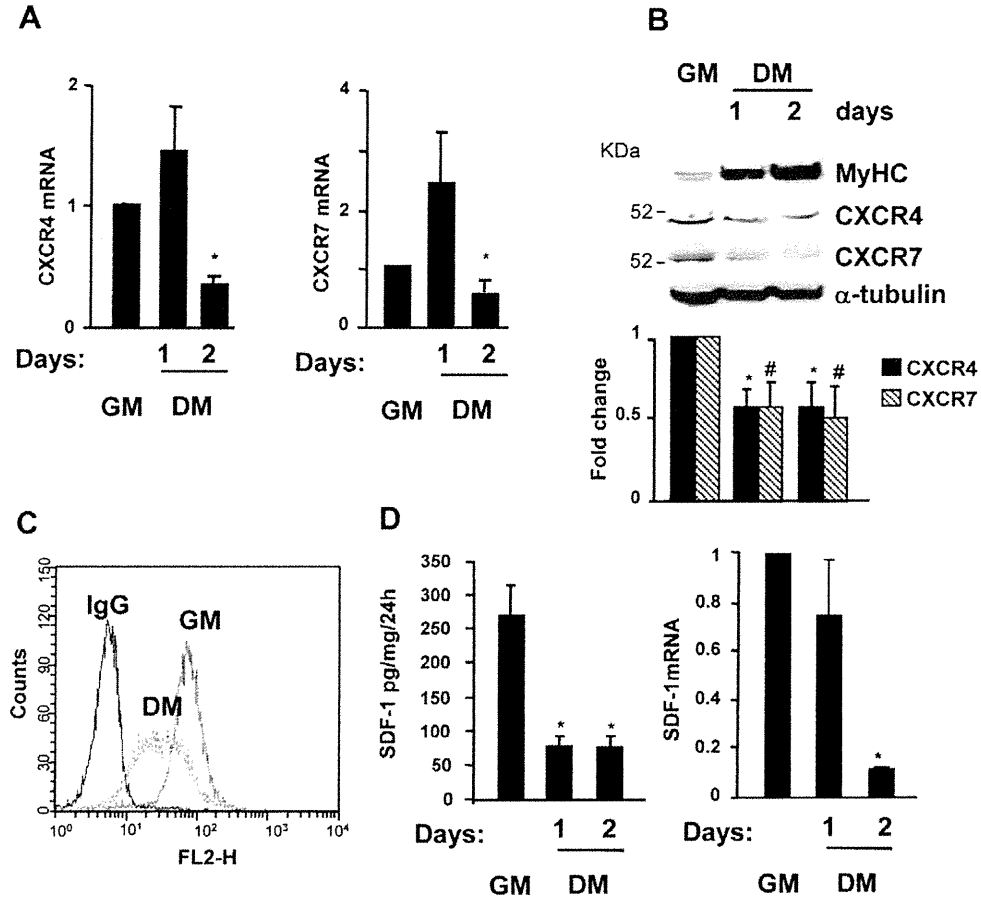

FIGURE 1. CXCR4, CXCR7, and SDF-1 expression decreases during myogenic differentiation. (**A**) Real-time PCR analysis of CXCR4 and CXCR7 expression in C2C12 cells cultured in growth medium (GM) and in differentiation medium (DM) for 1 and 2 days. $^{*}P < 0.05$ vs. GM and 1-day DM. (**B**) Western blot analysis of total cellular extracts from cells cultured as in (**A**) to analyze CXCR4 and CXCR7 expression. α-tubulin served as loading control. Shown is one representative experiment out of five. Lower panel: average results of densitometric analysis of Western blots. $^{*}P < 0.05$ and $^{\#}P < 0.05$ vs. their respective GM samples. (**C**) Flow cytometric analysis of CXCR4 expression in GM and 2-day DM-cultured C2C12 cells. Shown is one representative experiment out of three. (**D**) SDF-1 levels in GM- and DM-cultured C2C12 cells. Left panel: ELISA determination of SDF-1 protein levels in GM- and DM-cultured C2C12 cell conditioned medium. Culture medium was changed every day, and SDF-1 levels in conditioned media were determined at day 1 in GM and at days 1 and 2 in DM. Right panel: RT-PCR analysis of SDF-1 mRNA expression in C2C12 cultured as indicated previously. Results represent mean ± SE of three experiments. $^{*}P < 0.01$ vs. GM. [Color figure can be viewed in the online issue, which is available at www.interscience.wiley.com.]

μM) for the last 30 minutes and processed as previously described.[21] Propidium iodide was added to the final concentration of 10 μg/ml, and flow cytometry was performed (FACSCalibur; Becton and Dickinson).

Statistical Analysis. Data are expressed as mean ± SE. Student's two-tailed *t*-test was performed, and $P \leq 0.05$ was considered statistically significant.

RESULTS

SDF-1, CXCR4, and CXCR7 Are Expressed by Myoblast Precursor Cells and Decrease during Myogenic Differentiation. Myoblast precursor C2C12 cells were induced to proliferate in GM or differentiate into myotubes in the presence of DM. CXCR4 and CXCR7 expression was then evaluated by both quantitative RT-PCR (Fig. 1A) and Western blot (Fig. 1B). We found that both receptors were expressed in GM culture conditions and that their levels decreased in differentiated cells (Fig. 1A and B). CXCR4 inhibition in DM cells was also confirmed by fluorescein-activated cell sorting (FACS) analysis (Fig. 1C): C2C12 cells that expressed CXCR4 were 81 ± 7% in GM and decreased to 59 ± 5% after 48 hours in DM. In additional experiments we tested whether C2C12 cells released SDF-1 in the culture medium and, if so, whether SDF-1 levels in the CM varied during differentiation. CM was collected at the indicated time-points from growing and differentiating C2C12 cells and assayed for the presence of SDF-1 by ELISA (Fig. 1D, left panel). In GM, SDF-1 concentration was 270 ± 80 pg/mg of protein per 24 hours (Fig. 1D, left panel). After 2 days of culture in DM, SDF-1 levels decreased to 75 ± 30 pg/mg of protein per 24 hours. The inhibition of SDF-1 secretion paralleled a decrease in mRNA expression, as demonstrated by real-time PCR (Fig. 1D, right panel).

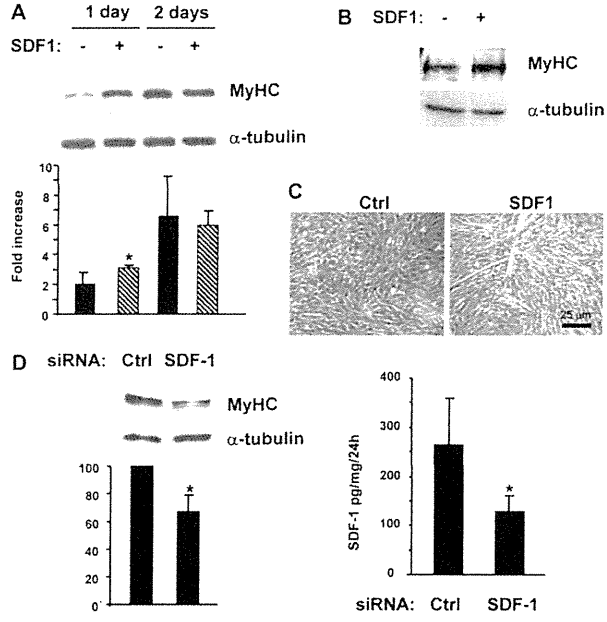

FIGURE 2. SDF-1 stimulates myogenic differentiation. Effect of SDF-1 on MyHC expression. At the switch from GM to DM, C2C12 cells (**A**) were treated with either 100 ng/ml SDF-1 (+) or left untreated (−) for 1–2 days and then analyzed by Western blot. Shown is one representative experiment out of six. Lower panel: average results of densitometric analysis of Western blots. $^*P < 0.05$ vs. untreated 1-day DM-cultured cells. (**B**) One representative experiment, out of three, showing the effect of treatment of satellite cells with SDF-1 for 1 day on MyHC expression. (**C**) Morphology of 1-day DM-cultured C2C12 cells in the presence of 100 ng/ml SDF-1. Cells were fixed and photomicrographs obtained by a Zeiss light microscope at ×20 magnification. (**D**) SDF-1 siRNA decreases MyHC levels in differentiating C2C12 cells. C2C12 cells were transfected either with control (Ctrl) or SDF-1 siRNA and transferred to DM for 48 hours. Left panel: cellular extracts were processed for Western blot to detect MyHC; average results of densitometric analysis of Western blots are also shown. Right panel: conditioned media of transfected cells were analyzed by ELISA to determine SDF-1 protein levels. $n = 3$; $^*P < 0.05$ vs. siRNA Ctrl transfected cells.

SDF-1 Anticipates Myogenic Differentiation. In these experiments, we evaluated whether SDF-1 affects myogenic differentiation. First, SDF-1 was added to DM culture medium of both C2C12 and primary satellite cells at a concentration of 100 ng/ml, and MyHC expression and myotube formation were evaluated. The administration of SDF-1 increased MyHC accumulation and myotube formation at day 1 in both C2C12 cells and satellite cells (Fig. 2A–C). Then, endogenous SDF-1 expression was knocked down by RNA interference. Proliferating C2C12 cells were transfected with either SDF-1 or control siRNAs and induced to differentiate in DM. After 48 hours, SDF-1–siRNA inhibited myogenic differentiation, as shown by reduced MyHC accumulation (Fig. 2D). The efficacy of siRNA-mediated SDF-1 knockdown was confirmed by the 53% reduction of SDF-1 levels in the culture medium of SDF-1–siRNA-transfected cells compared to cells transfected with control siRNA (Fig. 2D).

Myogenic Differentiation Occurs via both CXCR4 and CXCR7 Chemokine Receptors. To analyze the specific contribution of CXCR4 and CXCR7 in SDF-1–induced myogenic differentiation, in vitro experiments were performed aimed at inhibiting receptor activity. The addition of 10 μM 4FTN, a specific CXCR4 antagonist,[22] to DM culture medium of both C2C12 cells and satellite cells strongly inhibited MyHC accumulation (Fig. 3A) and myotube formation (Fig. 3B). Similar results were obtained when C2C12 cells were cultured either in presence of a second CXCR4 antagonist, AMD3100, or a neutralizing anti-CXCR4 antibody (Fig. 3C).

To inhibit CXCR7, two selective antagonists, CCX754[11] and CCX733, were used. Interestingly, both compounds reduced MyHC accumulation in DM-cultured C2C12 cells (Fig. 3D). These results were confirmed by targeting CXCR4 and CXCR7 with siRNA. Although C2C12 transfection with either CXCR4 or CXCR7 siRNAs did not result in a significant reduction of receptors (data not shown), MyHC protein levels were significantly lower in CXCR4 and CXCR7 siRNA-transfected cells compared to cells transfected with control siRNA (Fig. 3E).

These findings imply SDF-1 in myogenic differentiation through both CXCR4 and CXCR7 receptors.

To explain why the interference with the SDF-1/CXCR4 axis represses myogenic differentiation, levels of myogenic transcription factors were evaluated by reporter assay. As shown in Figure 4A, 4FTN-treated cells had significantly reduced levels of MyoD and myogenin compared with non-treated cells. Consistently, by report assay, we found that 4FTN significantly inhibited the expression of a luciferase reporter gene driven by the myosin creatine kinase promoter (Fig. 4B).

SDF-1 triggers multiple intracellular signals including p44/42 extracellular signal–regulated kinases (Erk1/2).[23] Moreover, Erk activation contributes to myogenic transcription and regulates post-mitotic responses.[24,25] Therefore, we tested whether SDF-1/CXCR4 controls myogenic differentiation by interfering with Erk signaling proteins. Western blot analysis performed with cellular extracts from 4FTN-treated C2C12 revealed a marked inhibition of Erk phosphorylation after 48-hour exposure of differentiating C2C12 to 4FTN (Fig. 4C).

The CXCR4 Antagonist 4FTN Inhibits Cell Cycle Withdrawal. As the inhibition of CXCR4 signaling yielded a more marked effect on myogenic

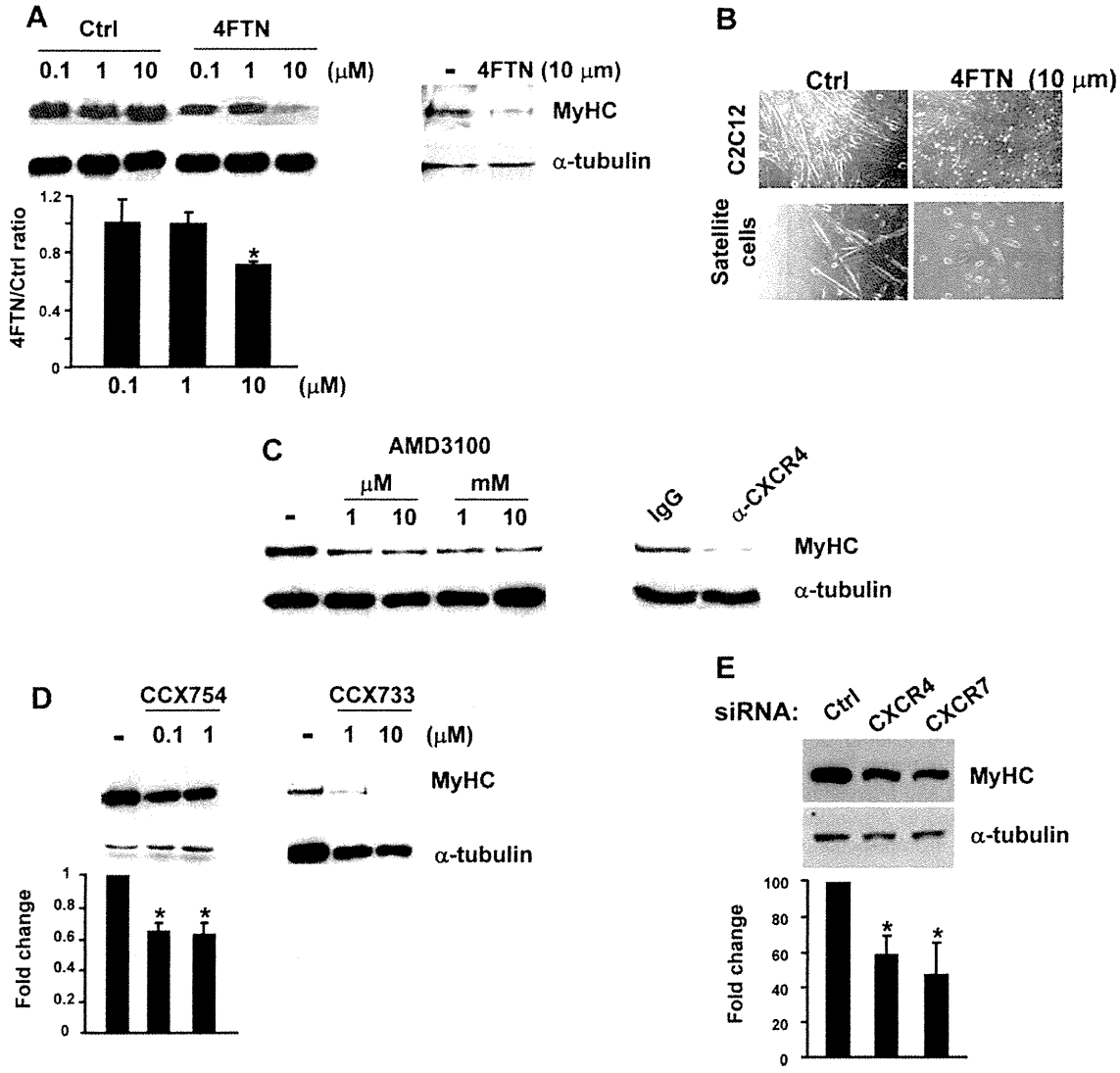

FIGURE 3. Both CXCR4 and CXCR7 antagonists inhibit myogenic differentiation. (**A, B**) The CXCR4 antagonist, 4FTN, inhibits MyHC accumulation and myotube formation in differentiating C2C12 cells and satellite cells. C2C12 cells (right panel) and satellite cells (left panel) were cultured in GM, transferred to DM, and grown for 48 hours in the presence of 4FTN or control peptide (Ctrl) at the indicated concentrations. Western blot analysis was performed on total cell extracts, and filters were probed with anti-MyHC antibody to monitor myogenic differentiation and anti–α-tubulin antibody for equal loading. Average results are shown for MyHC densitometric analysis for the experimental protocol shown in (**A**) as the ratio between 4FTN-treated cells and their respective untreated cells. (**B**) Representative experiment showing morphology of C2C12 and satellite cells cultured as in (**A**). Cells were fixed and photomicrographs obtained by a Zeiss light microscope at ×20 magnification. (**C**) Western blot analysis of total extracts from 48-hour DM-cultured C2C12 cells with the indicated concentration of CXCR4 inhibitor, AMD3100 (left panel), and 50 ng/ml of anti-CXCR4 or IgG antibodies (right panel). Shown is one representative experiment out of two. (**D**) Western blot analysis of DM-cultured C2C12 cells with CXCR7 inhibitors, CCX754 and CCX733. Lower panel: average results of densitometric analysis of CCX754 Western blots. $n = 3$; $^*P < 0.05$. For CCX733, one of two experiments is shown. (**E**) CXCR4 and CXCR7 siRNA decreases MyHC levels in differentiating C2C12 cells. Western blot analysis of C2C12 transfected with either CXCR4 or CXCR7 siRNAs and transferred to DM for 48 hours. Lower panel: average results of densitometric analysis of Western blots. $n = 3$; $^*P < 0.05$ vs. control siRNA transfected cells (Ctrl). All filters were probed with anti-MyHC antibody to monitor myogenic differentiation.

differentiation than CXCR7 antagonism, we further characterized the mechanisms underlying CXCR4-induced effects.

Therefore, we analyzed whether inhibition of CXCR4 signaling had an effect on C2C12 cell growth. Propidium iodide and BrdU staining followed by FACS analysis of cell cycle distribution revealed that 4FTN induced S-phase accumulation of DM-cultured C2C12 cells. After 18 hours of culture in the presence of 4FTN, the number of $BrdU^+$ cells increased from 15 ± 2.9% to 24.6 ± 3.7% in DM-cultured cells vs. 31.1 ± 2.8% in GM-cultured cells (Fig. 5A and B).

Given that 4FTN promoted proliferation and inhibited differentiation, we monitored the expression of pRb in C2C12 cells as Rb hypophosphorylation is necessary for growth arrest and myogenic program activation (Fig. 5C). As expected, in

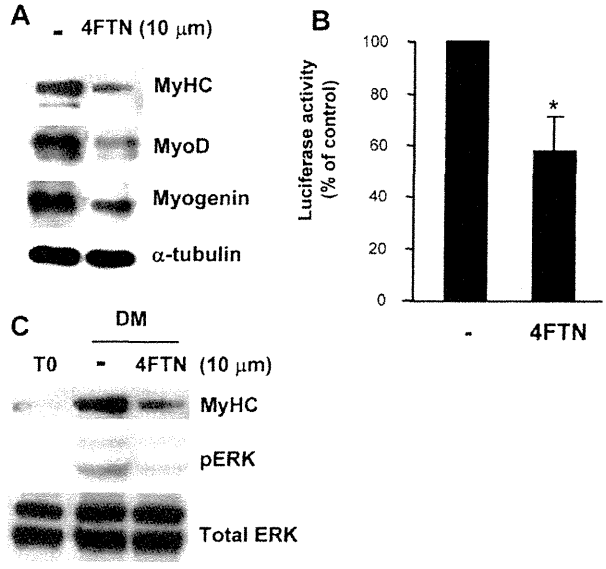

FIGURE 4. 4FTN represses MRF expression and p42/44 ERK phosphorylation. C2C12 cells were grown in DM for 2 days in the absence (−) or in the presence of 4FTN. Western blot analysis was performed with the indicated antibodies ($n = 2$). (**B**) C2C12 cells were transfected with pMCK-luciferase (0.5 μ g) and pCMV-β-Gal (0.5 μg). At 3 hours after transfection, cells were transferred in DM and cultured either in the absence (−) or presence of 4FTN for 24 hours. Then, cells were harvested for evaluation of luciferase and β-galactosidase activity. The values shown were normalized to β-galactosidase activity in order to correct for differences in transfection efficiency and are the average of three independent experiments ± SE, performed in triplicate. *$P < 0.01$ vs. untreated cells. (**C**) Western blot analysis of C2C12 treated as in (**A**) to detect Erk phosphorylation (pErk). Normalization of the lane was performed using the antibody directed against total Erk. T0 indicates GM-cultured cells.

proliferating C2C12 cells, pRb accumulated in its hyperphosphorylated inactive form (Fig. 5C, lane 1). When cells were induced to differentiate, pRb underwent dephosphorylation (Fig. 5C, lane 2). Interestingly, in the presence of 4FTN, pRb was less hypophosphorylated (Fig. 5C, lane 3).

Taken together these data suggest that inhibition of the SDF-1/CXCR4 axis blocks myogenic cell cycle withdrawal. Therefore, it was expected that the myogenic differentiation program should be temporarily inhibited by 4FTN. To verify this hypothesis, C2C12 cells were placed in DM in the presence of 4FTN for 2 days and then shifted to DM or GM in the absence of such compound. Removal of the CXCR4 antagonist resulted in MyHC accumulation (Fig. 5C, lane 4) and myotube formation (not shown) in the presence of DM. In contrast, when cells were placed in GM, myogenic differentiation did not occur, and cells acquired a proliferative phenotype and displayed pRb accumulation in its hyperphosphorylated form (Fig. 5C, lane 5). Therefore, inhibition of the CXCR4/SDF1 axis avoided the withdrawal of C2C12 from the cell cycle.

DISCUSSION

Skeletal muscle differentiation is a highly ordered process characterized by cell cycle withdrawal, muscle-specific gene expression, and myoblast fusion into multinucleated myotubes.[26] Myoblast differentiation is a process important not only in muscle physiology in response to fiber stress induced by injury, weight-bearing, or physical exercise, but also in pathological conditions. Signaling pathways that drive proliferation must be suppressed to allow induction of differentiation. These steps require the activation of muscle-regulatory transcription factors (MRFs), MyoD, myogenin, MRF4, and Myf5, and are tightly regulated by positive and negative mechanisms triggered by growth factors.[27]

SDF-1 is highly expressed in regenerating skeletal and cardiac muscle, where it plays a role in stem cell recruitment and vessel formation.[9,28] However, SDF-1 activity on satellite cells that are key players in promoting muscle fiber formation after injury has only been partially characterized in adult skeletal muscles. In this study we have addressed the question of whether SDF-1 could play a role in skeletal myogenesis.

We have shown that the myogenic murine cell line C2C12 expresses SDF-1 and its receptors CXCR4 and CXCR7, and that their expression levels are modulated during myogenic differentiation.

Growth factor receptor down-modulation with the onset of differentiation is required to ensure the irreversible withdrawal from the cell cycle and, consequently, the stable expression of muscle-specific phenotype.[27,29,30] Our studies suggest that CXCR4 and CXCR7 are associated with the proliferative state of myoblasts, because a reduction of these receptors was observed after induction of differentiation. Moreover, we showed that SDF-1 may act in the early phases of differentiation and hypothesized that the diminished levels of SDF-1 and its receptors at later time-points may represent a shut-off mechanism that concurs with the regulation of myogenic differentiation. Accordingly, we found that SDF-1 administration to differentiation medium anticipates MyHC accumulation and myotube formation in myoblasts: this effect was evident at 24 hours, whereas, at longer durations, myogenic differentiation proceeded independently of the presence of cytokine in the medium. Some reports have demonstrated that the SDF-1/CXCR4 axis is involved in myoblast migration and proliferation in vitro and in vivo[15,16,18,19,31]; however, its role in myogenic differentiation is controversial. A delay of differentiation of muscle progenitor cells has been reported following ectopic implants of SDF-1–expressing cells in the chicken embryo.[15] Similarly, a decrease of myogenic differentiation was observed by Odemis et al. when C2C12 myoblasts were cultured in the

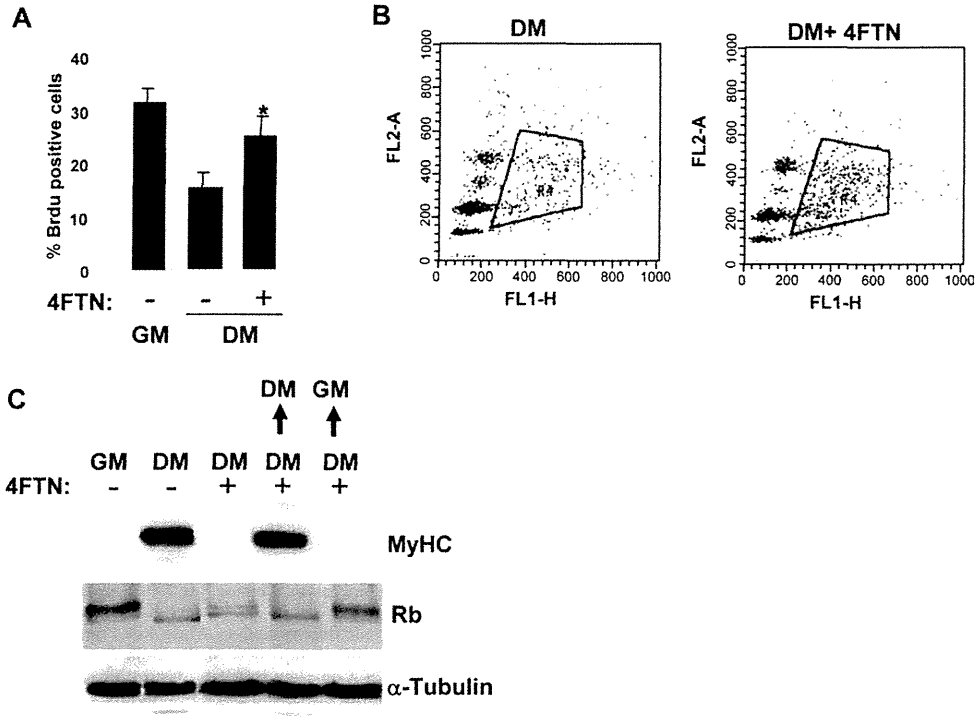

FIGURE 5. The CXCR4 antagonist, 4FTN, inhibits cell cycle withdrawal. (**A**) DM-cultured C2C12 cells were exposed to BrdU for 30 minutes following 1-day incubation with 4FTN. Cells were then stained with anti-BrdU MAb, quantified by FACS analysis, and expressed as percentage of BrdU-positive cells. Data represent the mean ± SE of four independent experiments (*$P < 005$). (**B**) Representative FACS analysis of cells cultured as in (**A**). (**C**) C2C12 cells were grown in DM in the presence (+) or absence (−) of 4FTN for 48 hours and then transferred to either DM or GM for 2 days in the absence of antagonist. Also shown are GM-cultured cells in the absence of 4FTN treatment (lane 1). Western blot analysis was performed and filters immunoblotted with the indicated antibodies. Cells kept in DM and treated with 4FTN (lane 3) showed, as expected, inhibition of myogenic differentiation. In contrast, MyHC was expressed in 4FTN-treated cells after removal of the CXCR4 antagonist (lane 4), which differed from cells shifted to GM (lane 5).

presence of 10 ng/ml SDF-1.[18] Different experimental conditions could account for the discrepancy of these data when compared with our observations. Moreover, a stimulation of myogenic differentiation by SDF-1 could follow a biphasic, concentration-dependent effect. Notably, insulin-like growth factor-1 (IGF-1) promotes differentiation at low doses, but it has an inhibitory effect at high doses.[32,33]

The involvement of SDF-1 in the positive regulation of myogenesis is further supported by our data showing that the inhibition of SDF-1 signaling in differentiation culture conditions avoided permanent withdrawal of myoblasts from the cell cycle and their differentiation. Indeed, the interference of SDF-1/CXCR4 and CXCR7 axes, either by drugs or by siRNAs, resulted in inhibition of MyHC accumulation in differentiating myoblasts. Further, in the presence of the CXCR4 inhibitor, 4FTN, p42/44 Erk phosphorylation was reduced, and the expression of muscle regulatory factors, including MyoD and myogenin, required to establish the irreversible commitment to terminal differentiation, was impaired. In agreement with our results, the inhibition of SDF-1/CXCR4 signaling in zebrafish, by morpholinos, induced a decrease in fast muscle formation and in MyoD and Myf5 expression.[34] Moreover, Yusuf et al. reported that CXCR4 signaling promoted migration and differentiation of myogenic progenitors in the chick limb.[31]

In conclusion, we have found that SDF-1 participates in muscle regeneration by promoting muscle progenitor/satellite cell differentiation, via both CXCR4- and CXCR7-induced signaling, with potential implications for the development of innovative treatments aimed at protecting muscle mass and function.

This work was supported by the Association Française contre les Myopathies (AFM), Grant 2007, Dossier No. 12558 (to R.M.). The first two authors (R.M. and A.D.C.) contributed equally to this article. We thank Professor N. Fujii and Dr. T. Schall for providing CXCR4 and CXCR7 antagonists, respectively.

REFERENCES

1. Nagasawa T, Hirota S, Tachibana K, Takakura N, Nishikawa S, Kitamura Y, et al. Defects of B-cell lymphopoiesis and bone-marrow myelopoiesis in mice lacking the CXC chemokine PBSF/SDF-1. Nature 1996;382:635–638.
2. Tachibana K, Hirota S, Iizasa H, Yoshida H, Kawabata K, Kataoka Y, et al. The chemokine receptor CXCR4 is essential for vascularization of the gastrointestinal tract. Nature 1998;393:591–594.
3. Zou YR, Kottmann AH, Kuroda M, Taniuchi I, Littman DR. Function of the chemokine receptor CXCR4 in haematopoiesis and in cerebellar development. Nature 1998;393:595–599.
4. Bagri A, Gurney T, He X, Zou YR, Littman DR, Tessier-Lavigne M, Pleasure SJ. The chemokine SDF1 regulates migration of dentate granule cells. Development 2002;129:4249–4260

5. Lu M, Grove EA, Miller RJ. Abnormal development of the hippocampal dentate gyrus in mice lacking the CXCR4 chemokine receptor. Proc Natl Acad Sci USA 2002;99:7090–7095.
6. Ma Q, Jones D, Borghesani PR, Segal RA, Nagasawa T, Kishimoto T, et al. Impaired B-lymphopoiesis, myelopoiesis, and derailed cerebellar neuron migration in CXCR4- and SDF-1-deficient mice. Proc Natl Acad Sci USA 1998;95:9448–9453.
7. Ara T, Tokoyoda K, Okamoto R, Koni PA, Nagasawa T. The role of CXCL12 in the organ-specific process of artery formation. Blood 2005;105:3155–3161.
8. Salvucci O, Yao L, Villalba S, Sajewicz A, Pittaluga S, Tosato G. Regulation of endothelial cell branching morphogenesis by endogenous chemokine stromal-derived factor-1. Blood 2002;99:2703–2711.
9. Abbott JD, Huang Y, Liu D, Hickey R, Krause DS, Giordano FJ. Stromal cell-derived factor-1alpha plays a critical role in stem cell recruitment to the heart after myocardial infarction but is not sufficient to induce homing in the absence of injury. Circulation 2004;110: 3300–3305.
10. Kapas S, Clark AJ. Identification of an orphan receptor gene as a type 1 calcitonin gene-related peptide receptor. Biochem Biophys Res Commun 1995;217:832–838.
11. Burns JM, Summers BC, Wang Y, Melikian A, Berahovich R, Miao Z, et al. A novel chemokine receptor for SDF-1 and I-TAC involved in cell survival, cell adhesion, and tumor development. J Exp Med 2006;203:2201–2213.
12. Miao Z, Luker KE, Summers BC, Berahovich R, Bhojani MS, Rehemtulla A, et al. CXCR7 (RDC1) promotes breast and lung tumor growth in vivo and is expressed on tumor-associated vasculature. Proc Natl Acad Sci USA 2007;104:15735–15740.
13. Sierro F, Biben C, Martinez-Munoz L, Mellado M, Ransohoff RM, Li M, et al. Disrupted cardiac development but normal hematopoiesis in mice deficient in the second CXCL12/SDF-1 receptor, CXCR7. Proc Natl Acad Sci USA 2007;104:14759–14764.
14. Mazzinghi B, Ronconi E, Lazzeri E, Sagrinati C, Ballerini L, Angelotti ML, et al. Essential but differential role for CXCR4 and CXCR7 in the therapeutic homing of human renal progenitor cells. J Exp Med 2008;205:479–490.
15. Vasyutina E, Stebler J, Brand-Saberi B, Schulz S, Raz E, Birchmeier C. CXCR4 and Gab1 cooperate to control the development of migrating muscle progenitor cells. Genes Dev 2005;19:2187–2198.
16. Odemis V, Lamp E, Pezeshki G, Moepps B, Schilling K, Gierschik P, et al. Mice deficient in the chemokine receptor CXCR4 exhibit impaired limb innervation and myogenesis. Mol Cell Neurosci 2005; 30:494–505.
17. Bae GU, Gaio U, Yang YJ, Lee HJ, Kang JS, Krauss RS. Regulation of myoblast motility and fusion by the CXCR4-associated sialomucin, CD164. J Biol Chem 2008;283:8301–8309.
18. Odemis V, Boosmann K, Dieterlen MT, Engele J. The chemokine SDF1 controls multiple steps of myogenesis through atypical PKCzeta. J Cell Sci 2007;120:4050–4059.
19. Ratajczak MZ, Majka M, Kucia M, Drukala J, Pietrzkowski Z, Peiper S, et al. Expression of functional CXCR4 by muscle satellite cells and secretion of SDF-1 by muscle-derived fibroblasts is associated with the presence of both muscle progenitors in bone marrow and hematopoietic stem/progenitor cells in muscles. Stem Cells 2003;21:363–371.
20. Rando TA, Blau HM. Primary mouse myoblast purification, characterization, and transplantation for cell-mediated gene therapy. J Cell Biol 1994;125:1275–1287.
21. Di Carlo A, De Mori R, Martelli F, Pompilio G, Capogrossi MC, Germani A. Hypoxia inhibits myogenic differentiation through accelerated MyoD degradation. J Biol Chem 2004;279:16332–16338.
22. Tamamura H, Fujisawa M, Hiramatsu K, Mizumoto M, Nakashima H, Yamamoto N, et al. Identification of a CXCR4 antagonist, a T140 analog, as an anti-rheumatoid arthritis agent. FEBS Lett 2004;569: 99–104.
23. Ganju RK, Brubaker SA, Meyer J, Dutt P, Yang Y, Qin S, et al. The alpha-chemokine, stromal cell-derived factor-1alpha, binds to the transmembrane G-protein-coupled CXCR-4 receptor and activates multiple signal transduction pathways. J Biol Chem 1998;273: 23169–23175.
24. Wu Z, Woodring PJ, Bhakta KS, Tamura K, Wen F, Feramisco JR, et al. p38 and extracellular signal-regulated kinases regulate the myogenic program at multiple steps. Mol Cell Biol 2000;20:3951–3964.
25. Bennett AM, Tonks NK. Regulation of distinct stages of skeletal muscle differentiation by mitogen-activated protein kinases. Science 1997;278:1288–1291.
26. Charge SB, Rudnicki MA. Cellular and molecular regulation of muscle regeneration. Physiol Rev 2004;84:209–238.
27. Florini JR, Ewton DZ, Magri KA. Hormones, growth factors, and myogenic differentiation. Annu Rev Physiol 1991;53:201–216.
28. Galvez BG, Sampaolesi M, Brunelli S, Covarello D, Gavina M, Rossi B, et al. Complete repair of dystrophic skeletal muscle by mesoangioblasts with enhanced migration ability. J Cell Biol 2006;174:231–243.
29. Florini JR, Magri KA. Effects of growth factors on myogenic differentiation. Am J Physiol 1989;256:C701–C711.
30. Olson EN. Interplay between proliferation and differentiation within the myogenic lineage. Dev Biol 1992;154:261–272.
31. Yusuf F, Rehimi R, Morosan-Puopolo G, Dai F, Zhang X, Brand-Saberi B. Inhibitors of CXCR4 affect the migration and fate of CXCR4+ progenitors in the developing limb of chick embryos. Dev Dyn 2006;235:3007–3015.
32. Florini JR, Ewton DZ, Falen SL, Van Wyk JJ. Biphasic concentration dependency of stimulation of myoblast differentiation by somatomedins. Am J Physiol 1986;250:C771–C778.
33. Engert JC, Berglund EB, Rosenthal N. Proliferation precedes differentiation in IGF-I-stimulated myogenesis. J Cell Biol 1996;135: 431–440.
34. Chong SW, Nguyet LM, Jiang YJ, Korzh V. The chemokine Sdf-1 and its receptor Cxcr4 are required for formation of muscle in zebrafish. BMC Dev Biol 2007;7:54.

5356 J. Med. Chem. 2010, 53, 5356–5360
DOI: 10.1021/jm1003528

Journal of
Medicinal
Chemistry
Brief Article

Peptide HIV-1 Integrase Inhibitors from HIV-1 Gene Products

Shintaro Suzuki,[†,#] Emiko Urano,[‡,#] Chie Hashimoto,[†] Hiroshi Tsutsumi,[†] Toru Nakahara,[†] Tomohiro Tanaka,[†] Yuta Nakanishi,[†] Kasthuraiah Maddali,[§] Yan Han,[‡] Makiko Hamatake,[‡] Kosuke Miyauchi,[‡] Yves Pommier,[§] John A. Beutler,[⊥] Wataru Sugiura,[‡] Hideyoshi Fuji,[∥] Tyuji Hoshino,[∥] Kyoko Itotani,[†] Wataru Nomura,[†] Tetsuo Narumi,[†] Naoki Yamamoto,[‡] Jun A. Komano,[‡] and Hirokazu Tamamura*[,†]

[†]*Department of Medicinal Chemistry, Institute of Biomaterials and Bioengineering, Tokyo Medical and Dental University, 2-3-10 Kandasurugadai, Chiyoda-ku, Tokyo 101-0062, Japan,* [‡]*AIDS Research Center, National Institute of Infectious Diseases, 1-23-1 Toyama, Shinjuku-ku, Tokyo 162-8640, Japan,* [§]*Laboratory of Molecular Pharmacology, Center for Cancer Research, National Cancer Institute, National Institutes of Health, Bethesda, Maryland 20892-4255,* [∥]*Department of Physical Chemistry, Graduate School of Pharmaceutical Sciences, Chiba University, 1-33 Yayoi-cho, Inage-ku, Chiba 263-8522, Japan, and* [⊥]*Molecular Targets Laboratory, Center for Cancer Research, National Cancer Institute, National Institutes of Health, Frederick, Maryland 21702.* [#] *These authors contributed equally to this work.*

Received March 17, 2010

Anti-HIV peptides with inhibitory activity against HIV-1 integrase (IN) have been found in overlapping peptide libraries derived from HIV-1 gene products. In a strand transfer assay using IN, inhibitory active peptides with certain sequential motifs related to Vpr- and Env-derived peptides were found. The addition of an octa-arginyl group to the inhibitory peptides caused a remarkable inhibition of the strand transfer and 3′-end-processing reactions catalyzed by IN and significant inhibition against HIV replication.

Introduction

Many antiretroviral drugs are currently available to treat human immunodeficiency virus type 1 (HIV-1) infection. Viral enzymes such as reverse transcriptase (RT[a]), protease and integrase (IN), gp41, and coreceptors are the main targets for antiretroviral drugs that are under development. Because of the emergence of viral strains with multidrug resistance (MDR), however, new anti-HIV-1 drugs operating with different inhibitory mechanisms are required. Following the success of raltegravir, IN has emerged as a prime target. IN is an essential enzyme for the stable infection of host cells because it catalyzes the insertion of viral DNA inside the preintegration complex (PIC) into the genome of host cells in two successive reactions, designated as strand transfer and 3′-end-processing. It is assumed that the enzymatic activities of IN have to be negatively regulated in the PIC during its transfer from the cytoplasm to the nucleus. Otherwise, premature activation of IN can lead to the autointegration into the viral DNA itself, resulting in an aborted infection. We speculate that the virus, rather than the host cells, must encode a mechanism to prevent autointegration. The PIC contains in association with the viral nucleic acid, viral proteins such as RT, IN, capsids ($p24^{CA}$ and $p7^{NC}$), matrix ($p17^{MA}$), p6 and Vpr, cellular proteins HMG I (Y), and the barrier to autointegration factor (BAF).[1−4] It is likely that, due to their spatial proximity in the PIC, these proteins physically and functionally interact with each other. For instance, it is already known that RT activity inhibited by Vpr,[5] and that RT and IN inhibit each other.[5−9] Vpr also inhibits IN through its C-terminal domain.[5,10] Because these studies suggest that PIC components regulate each other's function, we have attempted to obtain potent inhibitory lead compounds from a peptide fragment library derived from HIV-1 gene products, an approach which has been successful in finding a peptide IN inhibitor from LEDGF, a cellular IN binding protein.[11]

In this paper, we describe the screening of an overlapping peptide library derived from HIV-1 proteins, the identification of certain peptide motifs with inhibitory activity against HIV-1 IN, and the evaluation of effective inhibition of HIV-1 replication in cells using the identified peptide inhibitors possessing cell membrane permeability.

Results and Discussion

An overlapping peptide library spanning HIV-1 SF2 *Gag*, *Pol*, *Vpr*, *Tat*, *Rev*, *Vpu*, *Env*, and *Nef*, provided by Dr. Iwamoto of the Institute of Medical Science at the University of Tokyo (Supporting Information, SI, Figure 2A), was screened with a strand transfer assay[12] in search of peptide pools with inhibitory activity against HIV-1 IN. The library consists of 658 peptide fragments derived from the HIV-1 gene products. Each peptide is composed of 10−17 amino acid residues with overlapping regions of 1−7 amino acid residues. Sixteen peptide pools containing between 16 and 65 peptides were used for the first screening at the final concentration of 5.0 μM for each peptide (SI Figure 2B). This initial screening gave the results shown in Figure 1. Both Vpr and Env4 pools showed remarkable inhibition of IN strand transfer activity, and consequently a second screening was performed using the individual peptides contained in the Vpr and Env4 pools. A group of consecutive overlapping peptides in the Vpr pool (groups 13−15) and groups 4−6 and 20−21 in the Env4 pool were found to possess IN inhibitory activity (Figure 2). We focused on Vpr15 and Env4-4 peptides because they showed inhibitory activity against IN strand transfer reaction in a dose-dependent manner (Figure 3). The IC_{50} values of Vpr15

*To whom correspondence should be addressed. Phone: +81-3-5280-8036. Fax: +81-3-5280-8039. E-mail: tamamura.mr@tmd.ac.jp.

[a]Abbreviations: HIV, human immunodeficiency virus; IN, integrase; RT, reverse transcriptase; MDR, multidrug resistance; PIC, preintegration complex; BAF, barrier to autointegration factor; R_8, octa-arginyl.

 Published on Web 06/29/2010

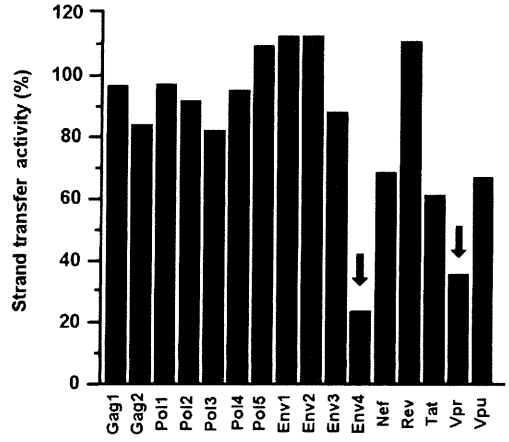

Figure 1. Inhibition of the IN strand transfer activity by peptide pools. Inhibition of the IN strand transfer activity was strongly inhibited by Env4 and Vpr pools (arrows). The *y*-axis represents the IN strand transfer activity relative to the solvent control (DMSO).

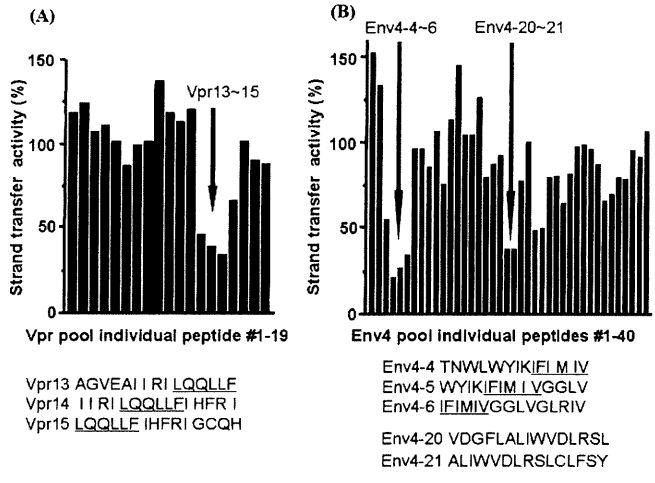

Figure 2. Identification of IN inhibitory peptides in the Vpr (A) and Env4 (B) pools based on the strand transfer activity of IN. The consecutive overlapping peptides display the inhibition of the strand transfer activity of IN (arrows). The *y*-axis represents the IN strand transfer activity relative to the solvent control (DMSO). The concentration of each peptide was 5 μM. The common sequences of individual peptides derived from Vpr and Env4 pools with anti-IN activity are underlined.

and Env4-4 were estimated at 5.5 and 1.9 μM, respectively. These peptides did not show any significant inhibitory activity against HIV-1 RT, suggesting that they might inhibit IN strand transfer reaction selectively.

The overlapping peptides of Vpr13-15 and Env4-4-6 have the vommon hexapeptide sequences LQQLLF and IFIMIV, respectively. The LQQLLF sequence covers positions 64−69 of Vpr, which is a part of the second helix of Vpr. The IFIMIV sequence corresponds to positions 684−689 of gp160, which is a part of the transmembrane domain of TM/gp41. These hexapeptides are thought to be critical to inhibition of IN activity. It was recently reported[5] that similar peptides derived from Vpr inhibit IN with IC_{50} values of 1−16 μM, which is consistent with our data. In this report,[5] the peptide motif was found to be 15 amino acid residues spanning LQQLLF from the overlapping Vpr peptide library. In our study, more precise mapping of inhibitory motif in Vpr peptides was achieved by identifying the shorter effective peptide motif. We focused on the Vpr-derived peptide, LQQLLF (Vpr-1) to develop potent inhibitory peptides. However, the expression of inhibitory activity against IN

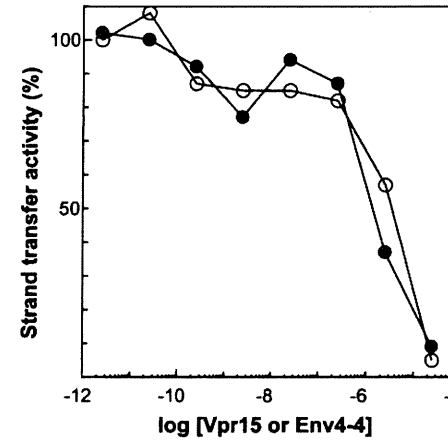

Figure 3. Concentration-dependent inhibition of IN strand transfer activities by Vpr15 (○) and Env4−4 (●) peptides. The *y*-axis represents the IN strand transfer activity relative to the solvent control (DMSO).

in vivo by only hexapeptides might be difficult because these hexapeptides penetrate the plasma membrane very poorly and to achieve antiviral activity, it is essential that they penetrate the cell membrane. To that effect, an octa-arginyl (R_8) group[13] was fused to the Vpr-derived peptides (Table 1). R_8 is a cell membrane permeable motif and its fusion with parent peptides successfully generates bioactive peptides without significant adverse effects or cytotoxicity.[14−18] In addition, the R_8-fusion could increase the solubility of Vpr-derived peptides which have a relatively hydrophobic character.

The inhibitory activity of Vpr-1 and Vpr-1-4 R_8 peptides against IN was evaluated based on the strand transfer and 3′-end-processing reactions in vitro (Table 1).[19,20] Vpr-1 did not show strong inhibition of either IN activity, but the IC_{50} of Vpr-1 R_8 toward the strand transfer reaction of IN was 10-fold lower than that of Vpr-1 lacking the R_8 group. This indicates that the positive charges derived from the R_8 group might enhance the inhibitory activity of the Vpr-1 peptide. Because we were concerned that the strong positive charges close to the LQQLLF motif might interfere with the inhibitory activity, the 6 amino acid sequence (−IHFRIG−) was inserted as a spacer between LQQLLF and R_8 (Vpr-3 R_8). The IHFRIG sequence was used to reconstitute the natural Vpr. The IC_{50} values of Vpr-2 R_8 for the strand transfer and 3′-end-processing activities of IN were 0.70 and 0.83 μM, respectively, while Vpr-3 R_8 showed potent IN inhibitory activities of 4.0 and 8.0 nM against the strand transfer and 3′-end- processing activities, respectively. This result indicates the additional importance of the IHFRIG sequence for inhibitory activities against IN. The increased IN inhibitory activities might be achieved presumably by the synergistic effect of the LQQLLF motif, the IHFRIG sequence, and the R_8 group. Vpr-4 R_8, in which the EAIIRI sequence was attached to further reconstitute the Vpr helix 2, showed inhibitory activities similar to those of Vpr-3 R_8, suggesting that reconstitution of helix 2 of Vpr is not necessary for efficient IN inhibition. Vpr-3 R_8 and Vpr-4 R_8, with $IC_{50} > 0.5\,\mu$M,[21] were less potent inhibitors of RT-associated RNase H activity, indicating that these peptides can selectively inhibit IN. These results suggest that Vpr-derived peptides are novel and distinct from any other IN inhibitors reported to date.

For rapid assessment of the antiviral effect of Vpr-derived peptides, we established an MT-4 Luc system in which MT-4 cells were stably transduced with the firefly luciferase expression cassette by a murine leukemia viral vector (SI Figure 3).

Table 1. Sequences of Vpr-Derived Peptides and Their IC_{50} Values toward the Strand Transfer and 3′-End Processing Reactions of IN

	sequence	IC_{50} (μM) strand transfer	IC_{50} (μM) 3′-end processing
Vpr-1	LQQLLF	68 ± 1.0	> 100
Vpr-1 R_8	Ac-LQQLLF -RRRRRRRR-NH_2	6.1 ± 1.1	> 11
Vpr-2 R_8	Ac-IHFRIG-RRRRRRRR-NH_2	0.70 ± 0.06	0.83 ± 0.07
Vpr-3 R_8	Ac-LQQLLF IHFRIG-RRRRRRRR-NH_2	0.004 ± 0.0001	0.008 ± 0.001
Vpr-4 R_8	Ac-EAIIRI LQQLLF IHFRIG-RRRRRRRR-NH_2	0.005 ± 0.002	0.006 ± 0.006

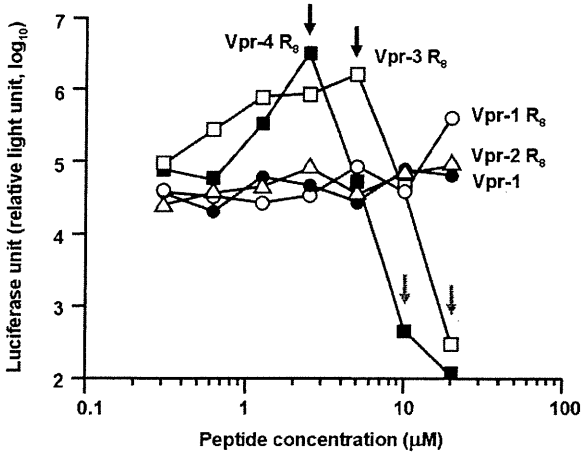

Figure 4. Luciferase signals in MT-4 Luc cells infected with HIV-1 in the presence of various concentrations of Vpr-derived peptides: Vpr-1 (●), Vpr-1 R_8 (○), Vpr-2 R_8 (△), Vpr-3 R_8 (□), Vpr-4 R_8 (■).

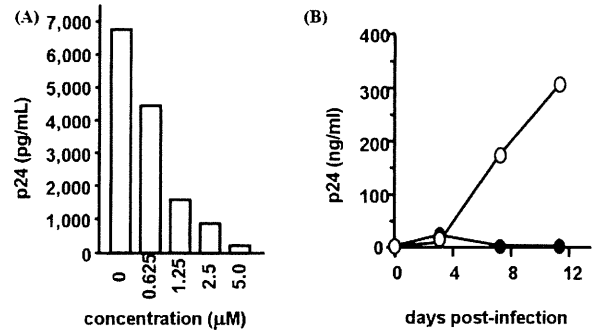

Figure 5. (A) The inhibition of HIV-$1_{JR\text{-}CSF}$ replication in NP2-CD4-CCR5 cells in the presence of various concentrations of Vpr-3 R_8. (B) The replication kinetics of HIV-1_{HXB2} in MT-4 cells in the presence of Vpr-3 R_8 (●). The concentration of Vpr-3 R_8 was fixed at 0.5 μM. Absence of Vpr-3 R_8 (○).

MT-4 Luc cells constitutively express high levels of luciferase which are significantly reduced by HIV-1 infection due to their high susceptibility to cell death upon HIV-1 infection. Protection of MT-4 Luc cells from HIV-1-induced cell death maintains the luciferase signals at high levels. In addition, the cytotoxicity of Vpr-derived peptides can be evaluated by a decrease of luciferase signals in these MT-4 Luc systems. Vpr-2 R_8, which is a weak IN inhibitor, showed no significant anti-HIV-1 activity below concentrations of 20 μM, suggesting that its moderate IC_{50} level in vitro is not sufficient to suppress HIV-1 replication in tissue culture and that the R_8 group is not significantly cytotoxic (Figure 4). Vpr-1 did not show any inhibitory effects against HIV-1 replication; however, Vpr-1 R_8 displayed a weak antiviral effect at a concentration of 20 μM and both Vpr-3 R_8 and Vpr-4 R_8 showed significant inhibitory effects against HIV-1 replication. The R_8 peptide did not show significant anti-HIV activity (IC_{50} > 50 μM, data not shown). These results suggest that the addition of the R_8 group enables Vpr-derived peptides to enter the cytoplasm and access IN, with the result that HIV-1 replication could be effectively inhibited.

Because Vpr-3 R_8 was less cytotoxic than Vpr-4 R_8, the inhibitory activities of Vpr-3 R_8 were further investigated. Two replication assay systems, R5-tropic HIV-$1_{JR\text{-}CSF}$ on NP2-CD4-CCR5 cells and X4-tropic HIV-1_{HXB2} on MT-4 cells, were utilized. NP2-CD4-CCR5 cells were infected with HIV-$1_{JR\text{-}CSF}$ in the presence of various concentrations of Vpr-3 R_8. On day 4 postinfection, the culture supernatant was collected and the concentration of viral p24 antigen was measured by an ELISA assay. The p24 levels decreased in a dose-dependent manner with increasing the concentration of Vpr-3 R_8; 50% inhibition of p24 expression was obtained with approximately 0.8 μM of Vpr-3 R_8 (Figure 5A). This concentration was approximately 10-fold lower than the concentration of Vpr-3 R_8 known to be cytotoxic (Figure 4). Second, MT-4 cells were infected with HIV-1_{HXB2} and the replication kinetics was monitored in the presence of 0.5 μM Vpr-3 R_8. The degree of replication of HIV-1_{HXB2} was quite low in the presence of Vpr-3 R_8, while replication of HIV-1_{HXB2} was robust in the absence of Vpr-3 R_8 (Figure 5B), suggesting that Vpr-3 R_8 strongly suppresses the replication of HIV-1 in cells. To examine whether the HIV-1 replication was blocked through the inhibition of IN activity, quantitative real-time PCR was performed. If IN is inhibited, the efficiency of viral genome integration should be decreased while the reverse transcription of viral genome should not be affected. Accordingly, NP2-CD4-CXCR4 cells were infected with HIV-1_{HXB2} in the presence or absence of 0.5 μM Vpr-3 R_8. Genomic DNA was extracted on day 2 postinfection, and the viral DNA was quantified at the various steps of viral entry phase. The level of "strong stop DNA", representing the total genome of infected virus in Vpr-3 R_8-treated cells, was similar (139.7%) to that in DMSO-treated control cells and the level of viral DNA generated at the late stage of reverse transcription in Vpr-3 R_8-treated cells was slightly decreased (84.4%) compared to control cells. This small decline can probably be attributed to the weak anti-RNase H activity of Vpr-3 R_8. On the other hand, a drastic decrease of Alu-LTR products was observed in Vpr-3 R_8-treated cells (15.8%), indicating an inhibition of integrated viral genome. Concomitantly, the double LTR products, representing the end-joined viral genome catalyzed by host cellular enzymes, were increased by a factor of 8 (779.8%). These results strongly suggest that Vpr-3 R_8 blocks viral infection by inhibiting IN activity in cells, consistent with our in vitro observations. Judging by these results, Vpr-derived peptides with the R_8 group are potent IN inhibitors that suppress HIV-1 replication in vivo.

Finally, in silico molecular docking simulations of Vpr-derived peptides and HIV-1 IN were performed. The Vpr-derived peptides are located in the second helix of Vpr and were thus considered to have an α-helical conformation.[22] Docking simulations of three peptides (Vpr13, Vpr14, and Vpr15), using the predicted structure of the HIV-1 IN dimer as a template,[23] were performed by GOLD software to investigate the binding mode of the peptides, the binding affinity of

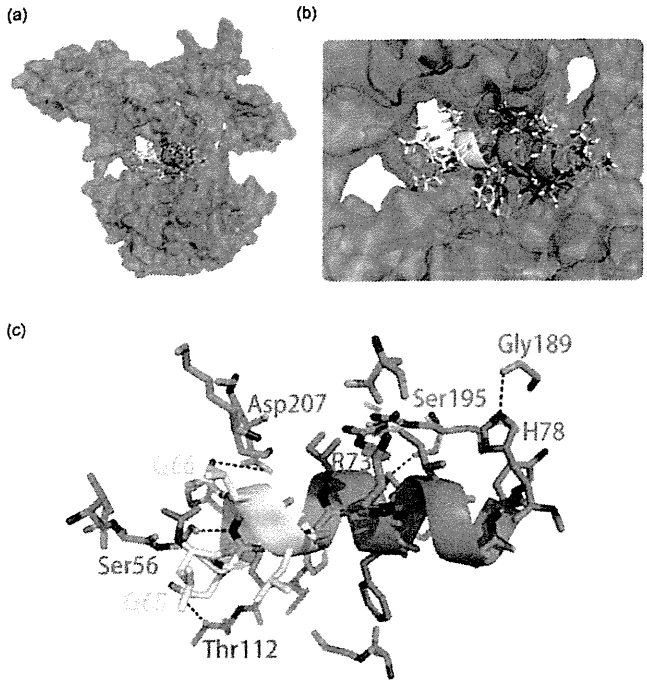

Figure 6. Predicted binding mode of Vpr15 to HIV-1 IN by GOLD. An overall view of (a) the complex obtained by docking Vpr15 with the HIV-1 IN dimer and (b) the closer view of the complex. The predicted structure of full-length HIV-1 IN was used as a template. Each HIV-1 IN monomer was shown as green or cyan surface. The docked Vpr15 is shown as a cartoon. The yellow-colored region is the LQQLLF motif. The GOLD score representing the docking complementarity is 69.83, indicating the high binding affinity between Vpr15 and IN. The hydrogen-bond interactions between HIV-1 IN and Vpr15 were presented by LIGPLOT software shown as blue dotted line (c).

the peptides being evaluated by GOLD Fitness score. The predicted binding mode of Vpr15 to IN is shown in Figure 6. Our results predict that the three Vpr-derived peptides interact with the cleft between the amino-terminal domain and the core domain of HIV-1 IN. This region is distinct from the nucleic acid interacting surfaces, indicating that the Vpr-derived peptides inhibit IN function in an allosteric manner. A previous report provided a model in which a Vpr peptide was bound to IN in a manner similar with our model[5] and, interestingly, the peptides were bound to IN with an exterior surface of Vpr. This earlier report that the full-length Vpr inhibits IN[10] strongly supports the predicted binding mode of Vpr15. Five hydrogen-bond interactions between HIV-1 IN and Vpr15 were identified by LIGPLOT analysis,[24] which invoked the following IN-Vpr amino acids: IN Thr112-Vpr Gln65, IN Ser56-Vpr Gln66, IN Asp207-Vpr Gln66, IN Ser195-Vpr Arg73, and IN Gly189-Vpr His78. The numbering of Vpr amino acids is based on the Vpr full-length coordinate, Figure 6. Additional hydrophobic contacts between IN and Vpr15 were found in which the following IN-Vpr amino acid pairs are involved: IN Lys211-Vpr Gln66, IN Pro109-Vpr Phe69, IN Arg262-Vpr His71, and IN Arg187-Vpr Gln77. These data indicate that the Gln65, Gln66, and Phe69 residues in Vpr-derived peptides play a major role in the interaction between IN and Vpr-derived peptides.

Conclusions

In summary, two peptide motifs, LQQLLF from Vpr and IFIMIV from Env4, possessing inhibitory activity against HIV-1 IN, were identified through the screening of overlapping peptide library derived from HIV-1 gene products. We initially speculate that HIV encodes a mechanism to prevent autointegration in the PIC because integration activity must be regulated until the virus infects cells. This speculation is supported by the finding that IN inhibitors exist in the viral PIC components. Vpr-derived peptides with the R_8 group showed remarkable inhibitory activities against the strand transfer and 3′-end-processing reactions catalyzed by HIV-1 IN in vitro. In addition, Vpr-3 R_8 and Vpr-4 R_8 were shown to inhibit HIV-1 replication with submicromolar IC_{50} values in cells using the MT-4 Luc cell system. In the quantitative analysis of p24 antigen, 50% inhibition of HIV-$1_{JR\text{-}CSF}$ replication was caused by approximately 0.8 μM of Vpr-3 R_8, and the replication of HIV-1_{HXB2} was extensively suppressed in the long term by Vpr-3 R_8 at 0.5 μM concentrations. Our finding suggest that these peptides could serve as lead compounds for novel IN inhibitors. Amino acid residues critical to the interaction of Vpr-derived peptides with IN were identified by our in silico molecular docking simulations, and suggests that more potent peptides[25] or peptidomimetic IN inhibitors represent a novel avenue for future small molecule inhibitors of IN and HIV integration.

Experimental Section

Peptide Synthesis. Vpr-derived peptides containing the R_8 group were synthesized by stepwise elongation techniques of Fmoc-protected amino acids on NovaSyn TGR resin. Coupling reactions were performed using 5.0 equiv of Fmoc-protected amino acid, 5.0 equiv of diisopropylcarbodiimide, and 5.0 equiv of 1-hydroxybenzotriazole monohydrate. Cleavage of peptides from resin and side chain deprotection were carried out with 10 mL of TFA in the presence of 0.25 mL of *m*-cresol, 0.75 mL of thioanisole, 0.75 mL of 1,2-ethanedithiol, and 0.1 mL of water as scavenger by stirring for 1.5 h. After filtration of the deprotected peptides, the filtrate was concentrated under reduced pressure, and crude peptides were precipitated in cooled diethyl-ether. All crude peptides were purified by RP-HPLC and identified by MALDI-TOFMS. Purities of all final compounds were confirmed (>95% purity) by analytical HPLC. Detailed data are provided in SI.

Enzyme Assays. The strand transfer assay for the first screening was performed as described previously.[12] The IN strand transfer and 3′-end-processing assays for peptide motif characterizations were performed as described previously.[19,20] RNase H activity was measured as described by Beutler et al.[21]

Replication Assays. For HIV-1 replication assays, 1×10^5 cells were incubated at room temperature for 30 min with an HIV-1 containing culture supernatant (ca. 0.2−50 ng p24) and then washed and incubated. Culture supernatants were collected at different time points, and then the cells were passaged if necessary. Levels of p24 antigen were measured using a Retro TEK p24 antigen ELISA kit, according to the manufacture's protocol. Signals were detected using an ELx808 microplate photometer.

For MT-4 Luc assays, MT-4 Luc cells (1×10^3 cells) grown in 96-well plates were infected with HIV-1_{XHB2} (ca. 0.2−10 ng p24) in the presence of varying concentrations of Vpr-3 R_8. At 6−7 d postinfection, cells were lysed and luciferase activity was measured using the Steady-Glo assay kits according to the manufacture's protocol. Chemiluminescence was detected with a Veritas luminometer.

Acknowledgment. We thank Prof. A. Iwamoto's group of the Institute of Medical Science at the University of Tokyo for the peptide libraries and Dr. M. Nicklaus from NCI/NIH for providing the modeled structure of full-length HIV-1 IN. T.T. is supported by JSPS research fellowships for young scientists.

This work was supported in part by Grant-in-Aid for Scientific Research from the Ministry of Education, Culture, Sports, Science, and Technology of Japan, and Health and Labor Sciences Research Grants from Japanese Ministry of Health, Labor, and Welfare. K.M. and Y.P. are supported by the Intramural Program of the National Cancer Institute, Center for Cancer Research.

Supporting Information Available: Additional experimental procedures including MS data and figures; HPLC charts of final compounds, explanation for HIV-1 genes and the peptide pools, and illustration of MT-4 Luc system. This material is available free of charge via the Internet at http://pubs.acs.org.

References

(1) Bukrinsky, M. I.; Haggerty, S.; Dempsey, M. P.; Sharova, N.; Adzhubei, A.; Spitz, L.; Lewis, P.; Goldfarb, D.; Emerman, M.; Stevenson, M. A nuclear-localization signal within HIV-1 matrix protein that governs infection of nondividing cells. *Nature* **1993**, *365*, 666–669.

(2) Miller, M. D.; Farnet, C. M.; Bushman, F. D. Human immunodeficiency virus type 1 preintegration complexes: studies of organization and composition. *J. Virol.* **1997**, *71*, 5382–5390.

(3) Farnet, C. M.; Bushman, F. D. HIV-1 cDNA integration: Requirement of HMG I(Y) protein for function of preintegration complexes in vitro. *Cell* **1997**, *88*, 483–492.

(4) Chen, H.; Engelman, A. The barrier-to-autointegration protein is a host factor for HIV type 1 integration. *Proc. Natl. Acad. Sci. U.S. A.* **1998**, *95*, 15270–15274.

(5) Gleenberg, I. O.; Herschhorn, A.; Hizi, A. Inhibition of the activities of reverse transcriptase and integrase of human immunodeficiency virus type-1 by peptides derived from the homologous viral protein R (Vpr). *J. Mol. Biol.* **2007**, *369*, 1230–1243.

(6) Gleenberg, I. O.; Avidan, O.; Goldgur, Y.; Herschhorn, A.; Hizi, A. Peptides derived from the reverse transcriptase of human immunodeficiency virus type 1 as novel inhibitors of the viral integrase. *J. Biol. Chem.* **2005**, *280*, 21987–21996.

(7) Hehl, E. A.; Joshi, P.; Kalpana, G. V.; Prasad, V. R. Interaction between human immunodeficiency virus type I reverse transcriptase and integrase proteins. *J. Virol.* **2004**, *78*, 5056–5067.

(8) Tasara, T.; Maga, G.; Hottiger, M. O.; Hubscher, U. HIV-1 reverse transcriptase and integrase enzymes physically interact and inhibit each other. *FEBS Lett.* **2001**, *507*, 39–44.

(9) Gleenberg, I. O.; Herschhorn, A.; Goldgur, Y.; Hizi, A. Inhibition of human immunodeficiency virus type-1 reverse transcriptase by a novel peptide derived from the viral integrase. *Arch. Biochem. Biophys.* **2007**, *458*, 202–212.

(10) Bischerour, J.; Tauc, P.; Leh, H.; De Rocquigny, H.; Roques, B.; Mouscadet, J. F. The (52–96) C-Terminal domain of Vpr stimulates HIV-1 IN-mediated homologous strand transfer of mini-viral DNA. *Nucleic Acids Res.* **2003**, *31*, 2694–2702.

(11) Hayouka, Z.; Rosenbluh, J.; Levin, A.; Loya, S.; Lebendiker, M.; Veprintsev, D.; Kotler, M.; Hizi, A.; Loyter, A.; Friedler, A. Inhibiting HIV-1 integrase by shifting its oligomerization equilibrium. *Proc. Natl. Acad. Sci. U.S.A.* **2007**, *104*, 8316–8312.

(12) Yan, H.; Mizutani, T. C.; Nomura, N.; Tanaka, T.; Kitamura, Y.; Miura, H.; Nishizawa, M.; Tatsumi, M.; Yamamoto, N.; Sugiura, W. A novel small molecular weight compound with a carbazole structure that demonstrates potent human immunodeficiency virus type-1 integrase inhibitory activity. *Antivir. Chem. Chemother.* **2005**, *16*, 363–373.

(13) Suzuki, T.; Futaki, S.; Niwa, M.; Tanaka, S.; Ueda, K.; Sugiura, Y. Possible existence of common internalization mechanisms among arginine-rich peptides. *J. Biol. Chem.* **2002**, *277*, 2437–2443.

(14) Wender, P. A.; Mitchell, D. J.; Pattabiraman, K.; Pelkey, E. T.; Steinman, L.; Rothbard, J. B. The design, synthesis, and evaluation of molecules that enable or enhance cellular uptake: Peptoid molecular transporters. *Proc. Natl. Acad. Sci. U.S.A.* **2000**, *97*, 13003–13008.

(15) Matsushita, M.; Tomizawa, K.; Moriwaki, A.; Li, S. T.; Terada, H.; Matsui, H. A high-efficiency protein transduction system demonstrating the role of PKA in long-lasting long-term potentiation. *J. Neurosci.* **2001**, *21*, 6000–6007.

(16) Takenobu, T.; Tomizawa, K.; Matsushita, M.; Li, S. T.; Moriwaki, A.; Lu, Y. F.; Matsui, H. Development of p53 protein transduction therapy using membrane-permeable peptides and the application to oral cancer cells. *Mol. Cancer Ther.* **2002**, *1*, 1043–1049.

(17) Wu, H. Y.; Tomizawa, K.; Matsushita, M.; Lu, Y. F.; Li, S. T.; Matsui, H. Poly-arginine-fused calpastatin peptide, a living cell membrane-permeable and specific inhibitor for calpain. *Neurosci. Res.* **2003**, *47*, 131–135.

(18) Rothbard, J. B.; Garlington, S.; Lin, Q.; Kirschberg, T.; Kreider, E.; McGrane, P. L.; Wender, P. A.; Khavari, P. A. Conjugation of arginine oligomers to cyclosporin A facilitates topical delivery and inhibition of inflammation. *Nature Med.* **2000**, *6*, 1253–1257.

(19) Marchand, C.; Zhang, X.; Pais, G. C. G.; Cowansage, K.; Neamati, N.; Burke, T. R., Jr.; Pommier, Y. Structural determinants for HIV-1 integrase inhibition by beta-diketo acids. *J. Biol. Chem.* **2002**, *277*, 12596–12603.

(20) Semenova, E. A.; Johnson, A. A.; Marchand, C.; Davis, D. A.; Tarchoan, R.; Pommier, Y. Preferential inhibition of the magnesium-dependent strand transfer reaction of HIV-1 integrase by alpha-hydroxytropolones. *Mol. Pharmacol.* **2006**, *69*, 1454–1460.

(21) Parniak, M. A.; Min, K. L.; Budihas, S. R.; Le Grice, S. F. J.; Beutler, J. A. A fluorescence-based high-throughput screening assay for inhibitors of HIV-1 reverse transcriptase associated ribonuclease H activity. *Anal. Biochem.* **2003**, *322*, 33–39.

(22) Morellet, N.; Bouaziz, S.; Petitjean, P.; Roques, B. P. NMR structure of the HIV-1 regulatory protein Vpr. *J. Mol. Biol.* **2003**, *327*, 215–227.

(23) Karki, R. G.; Tang, Y.; Burke, T. R., Jr.; Nicklaus, M. C. Model of full-length HIV-1 integrase complexed with viral DNA as template for anti-HIV drug design. *J. Comput.-Aided Mol. Des.* **2004**, *18*, 739–760.

(24) Wallace, A. C.; Laskowski, R. A.; Thormton, J. M. LIGPLOT—a program to generate schematic diagrams of protein ligand interactions. *Protein Eng.* **1995**, *8*, 127–134.

(25) Li, H.-Y.; Zawahir, Z.; Song, L.-D.; Long, Y.-Q.; Neamati, N. Sequence-based design and discovery of peptide inhibitors of HIV-1 integrase: insight into the binding mode of the enzyme. *J. Med. Chem.* **2006**, *49*, 4477–4486.

Bioorganic & Medicinal Chemistry 18 (2010) 6771–6775

Contents lists available at ScienceDirect

Bioorganic & Medicinal Chemistry

journal homepage: www.elsevier.com/locate/bmc

Peptidic HIV integrase inhibitors derived from HIV gene products: Structure–activity relationship studies

Shintaro Suzuki [a], Kasthuraiah Maddali [b], Chie Hashimoto [a], Emiko Urano [c], Nami Ohashi [a], Tomohiro Tanaka [a], Taro Ozaki [a], Hiroshi Arai [a], Hiroshi Tsutsumi [a], Tetsuo Narumi [a], Wataru Nomura [a], Naoki Yamamoto [c,d], Yves Pommier [b], Jun A. Komano [c], Hirokazu Tamamura [a,*]

[a] Institute of Biomaterials and Bioengineering, Tokyo Medical and Dental University, Chiyoda-ku, Tokyo 101-0062, Japan
[b] Laboratory of Molecular Pharmacology, Center for Cancer Research, National Cancer Institute, National Institutes of Health, Bethesda, MD 20892-4255, USA
[c] AIDS Research Center, National Institute of Infectious Diseases, Shinjuku-ku, Tokyo 162-8640, Japan
[d] Department of Microbiology, Yong Loo Lin School of Medicine, National University of Singapore, Singapore 117597, Singapore

ARTICLE INFO

Article history:
Received 28 June 2010
Revised 17 July 2010
Accepted 20 July 2010
Available online 25 July 2010

Keywords:
HIV integrase
Inhibitory peptide
Glu-Lys pairs
Ala-scan

ABSTRACT

Structure–activity relationship studies were conducted on HIV integrase (IN) inhibitory peptides which were found by the screening of an overlapping peptide library derived from HIV-1 gene products. Since these peptides located in the second helix of Vpr are considered to have an α-helical conformation, Glu-Lys pairs were introduced into the *i* and *i* + 4 positions to increase the helicity of the lead compound possessing an octa-arginyl group. Ala-scan was also performed on the lead compound for the identification of the amino acid residues responsible for the inhibitory activity. The results indicated the importance of an α-helical structure for the expression of inhibitory activity, and presented a binding model of integrase and the lead compound.

1. Introduction

Highly active anti-retroviral therapy (HAART), which involves a combination of two or three agents from two categories, reverse transcriptase inhibitors and protease inhibitors, has brought us remarkable success in the clinical treatment of HIV-infected and AIDS patients.[1] However, it has been accompanied by serious clinical problems including the emergence of viral strains with multidrug resistance (MDR), considerable adverse effects and nonetheless high costs. As a result, new categories of anti-HIV agents operating with mechanisms of action different from those of the above inhibitors are sought. HIV-1 integrase (IN) is a critical enzyme for the stable infection of host cells since it catalyzes the insertion of viral DNA into the genome of host cells, by means of strand transfer and 3′-end processing reactions and thus it is an attractive target for the development of anti-HIV agents. Recently, the first IN inhibitor, raltegravir (Merck),[2] has appeared in a clinical setting. It is assumed that the activity of IN must be negatively regulated during the translocation of the viral DNA from the cytoplasm to the nucleus to prevent auto-integration. The virus, as well as the host cells, must encode mechanism(s) to prevent auto-integration since the regulation of IN activity is critical for the virus to infect cells.[3] By screening a library of overlapping peptides derived from HIV-1 SF2 gene products we have found three Vpr-derived peptides, **1**, **2** and **3**, which possess significant IN inhibitory activity, indicating that IN inhibitors exist in the viral pre-integration complex (PIC).[4] The above inhibitory peptides, **1**, **2** and **3**, are consecutive overlapping peptides (Fig. 1). Compounds **4** and **5** are 12- and 18-mers from the original Vpr-sequence with the addition of an octa-arginyl group[5] into the C-terminus for cell membrane permeability, respectively. Compounds **4** and **5** have IN inhibitory activity and anti-HIV activity. Here, we report structure–activity relationship studies on these lead compounds for the development of more potent IN inhibitors.

2. Results and discussion

To determine which lead compound is most suitable for further experiments, five peptides **6–10**, which were elongated by one amino acid starting with compound **4** and extended ultimately to **5**, were synthesized (Fig. 2). Judging by the 3′-end processing and strand transfer reactions in vitro,[6] these peptides **4–10** had similar inhibitory potencies (Table 1). As a result, we concluded that 12 amino acid residues derived from the original Vpr-sequence are of sufficient for IN inhibitory activity, and any peptide among **4–10** is a suitable lead.

* Corresponding author.
E-mail address: tamamura.mr@tmd.ac.jp (H. Tamamura).

0968-0896/$ - see front matter © 2010 Elsevier Ltd. All rights reserved.
doi:10.1016/j.bmc.2010.07.050

1 AGVEAIIRILQQLLF
2 IIRILQQLLFIHFRI
3 LQQLLFIHFRIGCQH
4 Ac-LQQLLFIHFRIG-RRRRRRRR-NH_2
5 Ac-EAIIRILQQLLFIHFRIG-RRRRRRRR-NH_2

Figure 1. Amino acid sequences of compounds **1–5**. Compounds **1–3** are consecutive overlapping peptides with free N-/C-terminus. These were found by the IN inhibitory screening of a peptide library derived from HIV-1 gene products. Compounds **4** and **5** are cell penetrative leads of IN inhibitors.

4 Ac-LQQLLFIHFRIG-RRRRRRRR-NH_2
6 Ac-ILQQLLFIHFRIG-RRRRRRRR-NH_2
7 Ac-RILQQLLFIHFRIG-RRRRRRRR-NH_2
8 Ac-IRILQQLLFIHFRIG-RRRRRRRR-NH_2
9 Ac-IIRILQQLLFIHFRIG-RRRRRRRR-NH_2
10 Ac-AIIRILQQLLFIHFRIG-RRRRRRRR-NH_2
5 Ac-EAIIRILQQLLFIHFRIG-RRRRRRRR-NH_2

Figure 2. Amino acid sequences of compounds **6–10**, which are elongated by one amino acid from compound **4** to **5**.

Table 1
IC_{50} values of compounds **4–10** toward the 3′-end processing and strand transfer reactions catalyzed by HIV-1 IN

Compound	IC_{50} (μM)	
	3′-End processing	Strand transfer
4	0.13 ± 0.02	0.06 ± 0.01
5	0.09 ± 0.01	0.04 ± 0.01
6	0.10 ± 0.01	0.07 ± 0.01
7	0.13 ± 0.02	0.11 ± 0.01
8	0.26 ± 0.04	0.11 ± 0.03
9	0.11 ± 0.01	0.07 ± 0.01
10	0.08 ± 0.01	0.05 ± 0.01

Structural analysis showed that the Vpr-derived peptides, **1**, **2** and **3**, are located in the second helix of Vpr and were thus considered to have an α-helical conformation.[7] Compound **5** was adopted as a lead for the development of compounds with an increase in α-helicity since a longer peptide is likely to form a more stable α-helical structure than a shorter one. Initially, Glu (E) and Lys (K) were introduced in pairs into compound **5** at the i and $i+4$ positions. In general, such disposition of Glu-Lys pairs at i and $i+4$ positions is considered to cause an increase in α-helicity due to formation of an ionic interaction of a β-carboxy group of Glu and an ε-amino group of Lys. Several analogs of **5** with Glu-Lys pairs were synthesized by Fmoc-solid phase peptide synthesis (Fig. 3). In the inhibitory assay against the 3′-end processing and strand transfer reactions catalyzed by HIV-1 IN in vitro, compounds **11** and **15** showed more potent inhibitory activities than **5** (Table 2). Substitution of Glu-Lys for His^{14}-Gly^{18} or Ile^3-Leu^7 caused no decrease in IN inhibitory activity but a significant increase in activity, suggesting that Ile^3, Leu^7, His^{14} and Gly^{18} are not indispensable for activity. Substitution of Glu-Lys for Ala^2-Ile^6 or Gln^9-Ile^{13} caused a slight decrease in IN inhibitory activity against the 3′-end processing and strand transfer reactions (compounds **12** and **13**), indicating that Ala^2 and/or Ile^6, and Gln^9 and/or Ile^{13} are partly required for activity. Substitution of Glu-Lys for Ile^4-Gln^8 caused a 2–4-fold decrease in IN inhibitory activity against the 3′-end processing and strand transfer reactions (compound **14**), showing that Ile^4 and/or Gln^8 are essential for activity. Substitution of Glu-Lys for Leu^{11}-Phe^{15} caused an eightfold decrease in IN inhibitory activity against the 3′-end processing reaction and a 1.5-fold decrease in IN inhibitory activity against the strand transfer reaction (compound **16**), indicating that Leu^{11} and/or Phe^{15} are indispensable for activity, especially for inhibition against 3′-end processing. Compound **17** has two substitutions of Glu-Lys for His^{14}-Gly^{18} and for Ala^2-Ile^6, which are common to compounds **11** and **12**, respectively. A twofold decrease in both IN inhibitory activities of compound **17** is mostly due to the substitution for Ala^2-Ile^6 common to **12**, although **17** is slightly less active than **12** in both IN inhibitory assays.

1 5 10 15
5 Ac-EAIIRILQQLLFIHFRIG-RRRRRRRR-NH_2
11 Ac-EAIIRILQQLLFI*E*FRI*K*-RRRRRRRR-NH_2
12 Ac-E*E*IIR*K*LQQLLFIHFRIG-RRRRRRRR-NH_2
13 Ac-EAIIRILQ*E*LLF*K*HFRIG-RRRRRRRR-NH_2
14 Ac-EAI*E*RIL*K*QLLFIHFRIG-RRRRRRRR-NH_2
15 Ac-EA*E*IRI*K*QQLLFIHFRIG-RRRRRRRR-NH_2
16 Ac-EAIIRILQQL*E*FIH*K*RIG-RRRRRRRR-NH_2
17 Ac-E*E*IIR*K*LQQLLFI*E*FRI*K*-RRRRRRRR-NH_2

Figure 3. Amino acid sequences of compounds **11–17**, into which Glu-Lys pairs have been introduced.

Table 2
IC_{50} values of compounds **5** and **11–17** toward the 3′-end processing and strand transfer reactions catalyzed by HIV-1 IN

Compound	IC_{50} (μM)	
	3′-End processing	Strand transfer
5	0.09 ± 0.01	0.04 ± 0.01
11	0.05 ± 0.01	0.01 ± 0.001
12	0.12 ± 0.01	0.047 ± 0.01
13	0.14 ± 0.02	0.065 ± 0.01
14	0.23 ± 0.03	0.15 ± 0.002
15	0.04 ± 0.01	0.031 ± 0.01
16	0.71 ± 0.21	0.06 ± 0.004
17	0.18 ± 0.06	0.08 ± 0.02

Anti-HIV activity of these compounds was assessed by an MT-4 Luc system, in which MT-4 cells were stably transduced with the firefly luciferase expression cassette by a murine leukemia viral vector. MT-4 Luc cells constitutively express high levels of luciferase. HIV-1 infection significantly reduces luciferase expression due to the high susceptibility of MT-4 cells to HIV-1 infection. Protection of MT-4 Luc cells from HIV-1-induced cell death maintains the luciferase signals at high levels. In addition, the cytotoxicity of test compounds can be evaluated by a decrease of luciferase signals in these MT-4 Luc systems. The parent compound **5** showed significant anti-HIV activity at concentrations above 1.25 μM, as reported previously (Fig. 4).[4] Compound **15** showed a significant inhibitory effect against HIV-1 replication, and is thus comparable to compound **5**. Compounds **11**, **14** and **16** also displayed weak antiviral effects at concentrations of 2.5 and 5.0 μM and compounds **12**, **13** and **17** failed to show any significant anti-HIV activity. These results suggest that there is a positive correlation between IN inhibitory activity and anti-HIV activity of the compounds. None of these compounds showed significant cytotoxic effects at concentrations below 5.0 μM.

The structures of compounds **5** and **11–17** were assessed by CD spectroscopy. Because the aqueous solubility of these peptides is not high the peptides were dissolved in 0.1 M phosphate buffer, containing 50% MeOH at pH 5.6. The CD spectra suggest that the parent compound **5**, which has no Glu-Lys pair, forms a typical α-helical structure, and the other compounds, with the exception of **11** and **15**, form α-helical structures similarly (Fig. 5). The order of strength of α-helicity is **12**, **16** > **14** > **17** > **5** > **13**. Compounds **11** and **15** have no characteristic pattern, although IN inhibitory activities of both compounds are superior to that of the parent

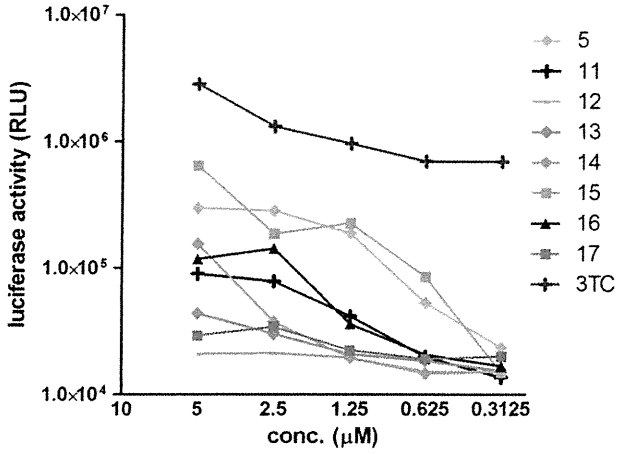

Figure 4. Luciferase signals in MT-4 Luc cells infected with HIV-1 in the presence of different concentrations of compounds **11–17**. Luciferase activity is expressed as relative luciferase units (RLU). 3TC is an HIV reverse transcriptase inhibitor, which was used as a positive control.

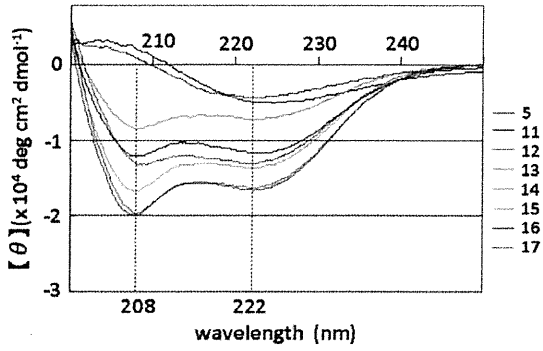

Figure 5. CD spectra of compounds **5** and **11–17** (5 μM) in 0.1 M phosphate buffer, pH 5.6 containing 50% MeOH at 25 °C.

compound **5**. Replacement of His^{14}-Gly^{18} and Ile^{3}-Leu^{7} by Glu-Lys in compounds **11** and **15**, respectively, caused a significant decrease in α-helicity, possibly due to formation of unfavorable salt bridges such as Glu^{14}-Arg^{16} and Glu^{3}-Arg^{5}. Introduction of a Glu-Lys pair into Gln^{9}-Ile^{13} in compound **13** caused a slight decrease in α-helicity, possibly due to interference in the formation of a salt bridge of Glu^{1}-Arg^{5} by that of Arg^{5}-Glu^{9}. In the other analogs, increases in α-helicity were observed to result from the introduction of Glu-Lys pairs as we had initially postulated. Overall, there is no positive correlation between IN inhibitory or anti-HIV activity and the degree of α-helicity of the compounds.

In order to identify the amino acid residues responsible for IN inhibitory and anti-HIV activities of these peptides, an Ala-scan of compound **4** was performed (Fig. 6). Compounds **18–22**, **25**, **27** and **29** showed IN inhibitory activities against the 3′-end processing and strand transfer reactions similar to those of **4** (Table 3). Ala-substitution for Leu^{7}, Gln^{8}, Gln^{9}, Leu^{10}, Leu^{11}, His^{14}, Arg^{16} or Gly^{18} did not cause any significant change in either of IN inhibitory activities, indicating that the replaced amino acids are not essential for IN inhibition. Ala-substitution for Phe^{12}, Ile^{13}, Phe^{15} or Ile^{17} gave compounds **23**, **24**, **26** and **28**, which were 2–4 times less active in both the IN inhibitory assays, suggesting that Phe^{12}, Ile^{13}, Phe^{15} and Ile^{17} are indispensable for IN inhibition. Assessment of anti-HIV activity in the MT-4 Luc system showed that all compounds **18–29** produced dose-dependent inhibition of HIV-1 replication, although they displayed cytotoxicity at 10 μM (**4**, **19–23**, **26** and **27**) or above 5 μM (**24** and **25**) (Fig. 7). Compounds **23** and **24**,

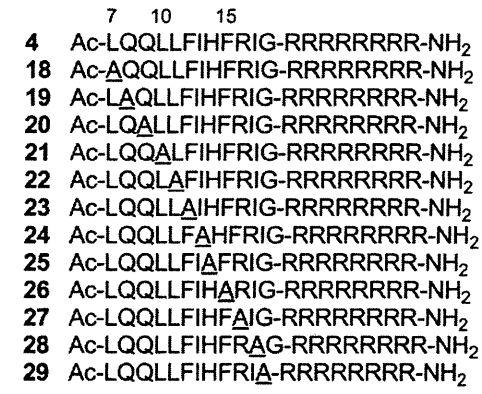

Figure 6. Amino acid sequences of compounds **18–29** based on an Ala-scan of compound **4**. Position numbers correspond to alignment with compound **5**.

Table 3
IC_{50} values of compounds **18–29** toward the 3′-end processing and strand transfer reactions catalyzed by HIV-1 IN

Compound	IC_{50} (μM)	
	3′-End processing	Strand transfer
4	0.11 ± 0.03	0.05 ± 0.01
18	0.12 ± 0.004	0.08 ± 0.01
19	0.13 ± 0.02	0.06 ± 0.01
20	0.10 ± 0.004	0.06 ± 0.01
21	0.12 ± 0.02	0.07 ± 0.01
22	0.13 ± 0.003	0.06 ± 0.01
23	0.34 ± 0.06	0.18 ± 0.03
24	0.33 ± 0.02	0.22 ± 0.01
25	0.13 ± 0.01	0.06 ± 0.01
26	0.25 ± 0.02	0.12 ± 0.01
27	0.11 ± 0.01	0.05 ± 0.01
28	0.20 ± 0.03	0.16 ± 0.02
29	0.09 ± 0.01	0.09 ± 0.01

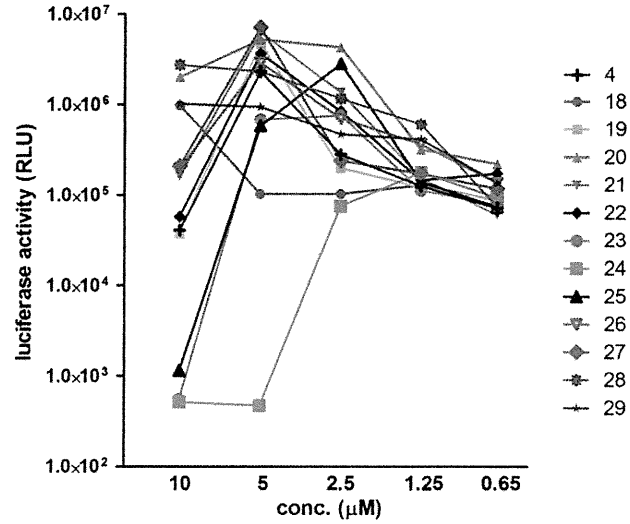

Figure 7. Luciferase signals in MT-4 Luc cells infected with HIV-1 in the presence of various concentrations of compounds **18–29**. Luciferase activity was valued as RLU.

with Ala-substitution for Phe^{12} and Ile^{13}, respectively, showed weaker inhibitory activity than **4** at 5 μM. Consequently, Phe^{12} and Ile^{13} were deemed to be critical for activity, which is consistent with the IN inhibitory activity results. A control peptide isomer of **5** (Ac-QIFEHLAGIIQILRFLRI-R_8-NH_2) did not show anti-HIV activity at

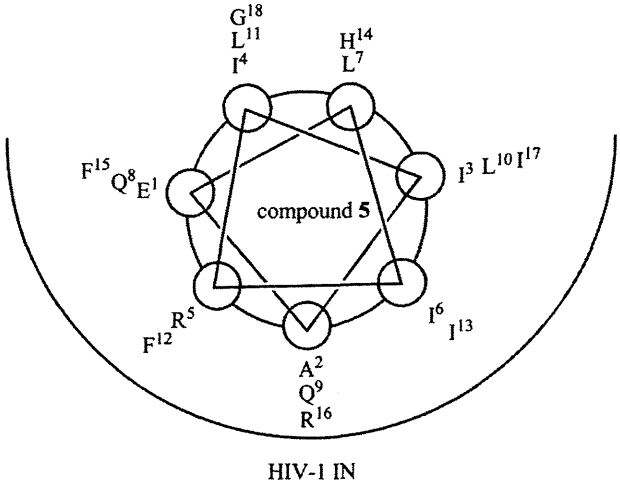

Figure 8. Brief presumed drawing of the binding model of HIV-1 IN and compound **5**.

concentrations below 10 μM, suggesting that the original Vpr-sequence, with the exceptions of Phe^{12}, Ile^{13}, Phe^{15} and Ile^{17}, is critical for activity.

The assumption that compound **5** forms an α-helical structure when binding to HIV-1 IN suggests the binding model of IN and **5** shown in Figure 8, as **5** forms an α-helical structure in 50% aqueous MeOH solution. In this model, Phe^{12}, Ile^{13}, Phe^{15} and Ile^{17}, which were identified by the Ala-scan experiment as critical residues, are located in the pocket of IN. His^{14} and Gly^{18}, which can be replaced by Glu-Lys with an increase of activity in compound **11**, are located outside of the pocket of IN. Ile^{3} and Leu^{7} can also be replaced by Glu-Lys while retaining activity in compound **15**, and Leu^{7} is located outside of the pocket, whereas Ile^{3} is located in the edge of the pocket. Compounds **11** and **15** might form α-helical structures when binding to IN, although **11** or **15** does not show α-helicity in the CD spectrum. Thus, these compounds might retain IN inhibitory activity. This binding model is compatible with the results of structure–activity relationship studies involving Glu-Lys substitution and Ala-scan. The reason for decreases in IN inhibitory and anti-HIV activity of compounds **12** and **17**, which show increases of α-helicity, are possibly due to substitution of Glu-Lys for Ala^{2} and Ile^{6}, which are located in the pocket of IN. The reason for a decrease in activity of compounds **14** and **16**, which show increased α-helicity, might be due to substitution of Lys for Gln^{8} and Phe^{15}, respectively, which are located in the pocket of IN. The reason for decreases in IN inhibitory and anti-HIV activity of compound **13**, which also shows a decrease of α-helicity, are possibly due to substitution of Glu-Lys for Gln^{9} and Ile^{13}, which are located in the pocket of IN.

3. Conclusion

In the present study, structure–activity relationship studies were performed on Vpr-derived peptides **4** and **5**, which had been previously identified as HIV-1 IN inhibitors.[4] The Glu-Lys substitution experiments and Ala-scan data suggest that several amino acid residues of **4** and **5** are indispensable for IN inhibitory and anti-HIV activities, and a binding model of IN and **5** were proposed. Furthermore, two novel compounds **11** and **15**, which contained Glu-Lys pairs and showed more potent IN inhibitory activities than compound **5**, were found. These data including the binding model should be useful for the development of potent HIV-1 IN inhibitors based on Vpr-peptides.

4. Experimental

4.1. Chemistry

All peptides were synthesized by the Fmoc-based solid-phase method. The synthetic peptides were purified by RP-HPLC and identified by ESI-TOF-MS. Fmoc-protected amino acids and reagents for peptide synthesis were purchased from Novabiochem, Kokusan Chemical Co., Ltd and Watanabe Chemical Industries, Ltd. Protected peptide resins were constructed on NovaSyn TGR resins (0.26 meq/g, 0.025 and 0.0125 mmol scales for Glu-Lys substitution and Ala-scan peptides, respectively). All peptides were synthesized by stepwise elongation techniques. Each cycle involves (i) deprotection of an Fmoc group with 20% (v/v) piperidine/DMF (10 mL) for 15 min and (ii) coupling with 5.0 equiv of Fmoc-protected amino acid, 5.0 equiv of diiopropylcarbodiimide (DIPCI) and 5.0 equiv of 1-hydroxybenzotriazole monohydrate (HOBt·H_2O) in DMF (3 mL) for 90 min. N-Terminal α-amino groups of Glu-Lys substitution and Ala-scan peptides were acetylated with 100 equiv of acetic anhydride in DMF (10 mL). Cleavage from the resin and side chain deprotection were carried out by stirring for 1.5 h with *m*-cresol (0.25 mL), thioanisole (0.75 mL), 1,2-ethanedithiol (0.75 mL) and TFA (8.25 mL). After removal of the resins by filtration, the filtrate was concentrated under reduced pressure, the crude peptides were precipitated in cooled diethyl ether and purified by preparative RP-HPLC on a Cosmosil 5C18-AR II column (10 × 250 mm, Nacalai Tesque, Inc.) with a LaChrom Elite HTA system (Hitachi). The HPLC solvents employed were water containing 0.1% TFA (solvent A) and acetonitrile containing 0.1% TFA (solvent B). All peptides were purified using a linear gradient of solvents A and B over 30 min at a flow rate of 3 cm^3 min^{-1}. The purified peptides were identified by ESI-TOF-MS (Brucker Daltonics micrOTOF-2focus) (shown in Table S1 in Supplementary data). All peptides were obtained after lyophilization as fluffy white powders of the TFA salts. The purities of these peptides were checked by analytical HPLC on a Cosmosil 5C18-ARII column (4.6 × 250 mm, Nacalai Tesque, Inc.) eluted with a linear gradient of solvents A and B at a flow rate of 1 cm^3 min^{-1}, and eluted products were detected by UV at 220 nm (shown in Figs. S1–S3 in Supplementary data).

4.2. Expression and purification of F185K/C280S HIV-1 integrase from *Escherichia coli*

Plasmid encoding IN1–288/F185K/C280S was expressed in *Escherichia coli* strain C41. The solubility of the mutant protein was examined in a crude cell lysate, as follows. Cells were grown in 1 L of culture medium containing 100 μg/mL of ampicillin at 37 °C until the optical density of the culture at 600 nm was between 0.4 and 0.9. Protein expression was induced by the addition of isopropyl-1-thio-β-D-galactopyranoside to a final concentration of 0.1 mM. After 2 h, the cells were collected by centrifugation at 6000 rpm for 30 min. After removal of the supernatant, the cells were resuspended in HED buffer (20 mM HEPES, pH 7.5, 1 mM EDTA, 1 mM DTT) with 0.5 mg/mL lysozyme and stored on ice for 30 min. The cells were sonicated until the solution exhibited minimal viscosity then it was centrifuged at 15,000 rpm for 30 min. After removal of the supernatant, the pellet was dissolved in TNM buffer (20 mM Tris/HCl, pH 8.0, 1 M NaCl, 2 mM 2-mercaptoethanol) with 5 mM imidazole and stored on ice for 30 min. The cells were then centrifuged at 15,000 rpm for 30 min and the supernatant was collected. The supernatant was then filtered through 0.45 μm filter cartridge and applied to a HisTrap column at 1 mL/min flow rate. After loading, the column was washed with 10 volume of TNM buffer with 5 mM imidazole. Protein was eluted with a linear gradient of 500 mM imidazole, containing TNM buf-